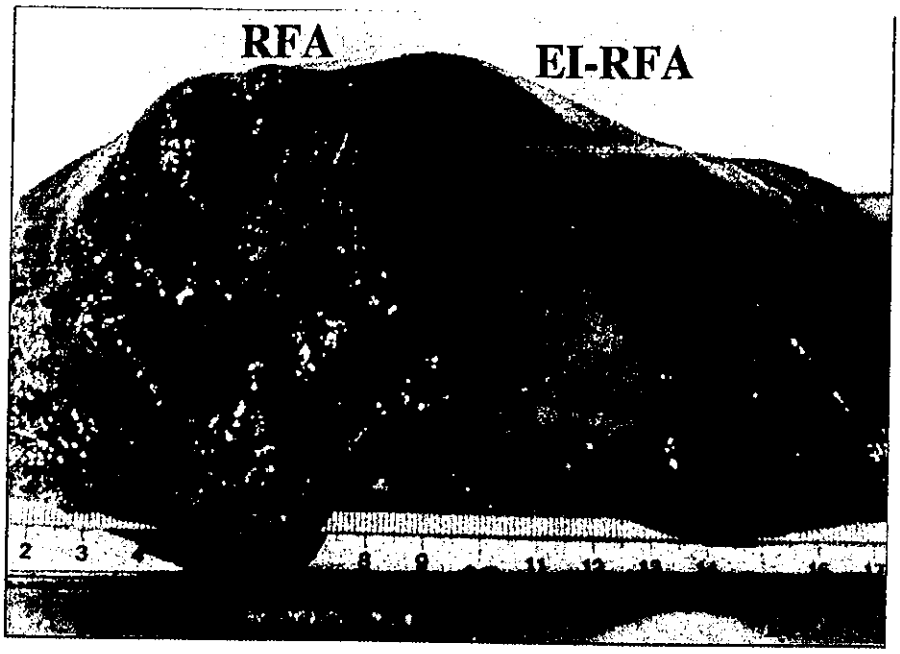

Figure 2. Liver specimen cut in the plane of the inserted electrodes after ablation using RITA. RFA (left side) created an elliptical whitish yellow area of apparent cell death. The ablation zone was increased in size by EI-RFA (right side), and the shape of the ablated area became rounder with EI-RFA.

after setting 130 W power during RFA using Radionics. The current density (ampere/cm^2) at the grand pat was measured as dividing a sum of peak current by 189 cm^2 that is an area covering external grand pat. As imaginary part of impedance of the liver tissue is <3% of total impedance at ablation frequency of 450 kIIz, real part of impedance is used as approximately measurable impedance.

For RITA, RFA was started at 20 W and accelerated by 10 W per min until the temperature reached 80°C. There was no system for recording total energy administered while adjusting the temperature when it reached over 80°C. Therefore, the total energy administered (joule) could not be accurately estimated in RITA.

Pathological examination. All liver specimens, including the margin of the ablated zone, were examined for pathological changes immediate after RFA and EI-RFA. Hematoxylin and eosin stain, silver staining, and Azan-Mallory staining were performed. The pathological features of the specimen treated with RFA (n=20) were compared with those of specimens treated with EI-RFA (n=20).

Statistical analysis. Data are expressed as the mean ± SD. Inter-group differences were assessed with an unpaired t-test (either Student's t-test or Welch's t-test) or the χ^2 test. The Kruskal-Wallis test was used to present significant differences between the 3 study groups. A $p<0.05$ was considered to be statistically significant.

Table I. The area of thermal ablation zone as determined by gross pathology.

	RFA alone	EI-RFA	p-value
Radionics (n=6)			
Longest diameter (cm)	3.2±0.4	4.2±0.5	0.0029[a]
Shortest diameter (cm)	3.0±0.4	3.7±0.4	0.0123[a]
Height (cm)	4.1±0.5	4.3±0.2	0.2464
Volume (cm^3)	23.2±7.7	35.3±7.4	0.0199[a]
RITA (n=7)			
Longest diameter (cm)	3.6±0.4	4.1±0.5	0.0543
Shortest diameter (cm)	3.1±0.3	3.8±0.4	0.0028[a]
Height (cm)	3.2±0.6	3.4±0.5	0.1553
Volume (cm^3)	19.7±4.7	30.7±10.3	0.0334[a]
RTC (n=7)			
Longest diameter (cm)	4.0±0.5	3.8±0.4	0.3705
Shortest diameter (cm)	3.1±0.7	2.9±0.9	0.6372
Height (cm)	3.1±0.4	2.4±0.5	0.0195[a]
Volume (cm^3)	19.9±5.8	15.6±7.7	0.2455

The size of the ablation zone achieved with EI-RFA was greater than that achieved with RFA using Radionics and RITA equipment. [a]Statistically significant ($p<0.05$).

Results

Ablation zone. Macroscopically, RFA created a well-circumscribed elliptical whitish yellow area of apparent cell death (Fig. 2). Diameters and volumes of thermal ablation zone as determined by gross pathology induced by RFA and EI-RFA are shown in Table I. The shortest diameter of the ablated zone of EI-RFA was greater than that of RFA alone when using either Radionics or RITA equipment (Radionics, 3.7±0.4 cm vs 3.0±0.4 cm; $p<0.05$), (RITA, 3.8±0.4 cm vs 3.1±0.3 cm; $p<0.01$). The longest diameter of the ablated

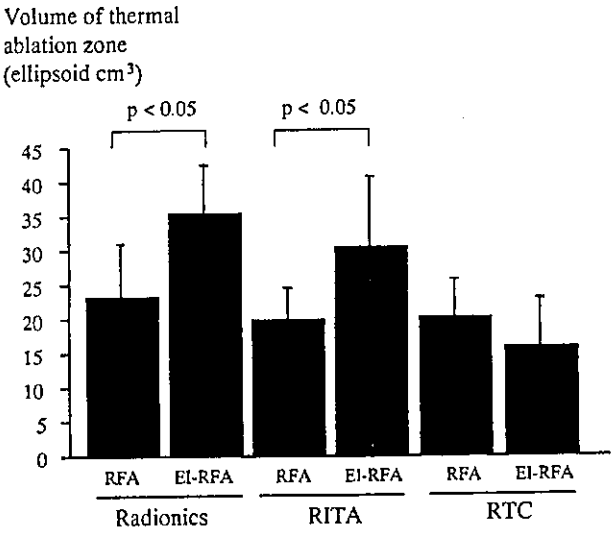

Figure 3. Volume of thermal ablation zone of RFA and of EI-RFA. The ablated volume obtained with EI-RFA was greater than that obtained with RFA using Radionics equipment (p=0.0199) and RITA (p=0.0334).

zone of EI-RFA was greater than that of RFA alone when using Radionics (3.2±0.4 cm vs 4.2±0.5 cm; p<0.01). No inter-group differences of the area of the ablation zone were observed depending on the equipment used to perform RFA alone, but the size of ablation zone caused by EI-RFA was greater with Radionics than with RTC (p<0.01). Also, the size of the zone caused by EI-RFA was greater with RITA than with RTC (p<0.01). The size of the ablation zone achieved with EI-RFA was greater than that achieved with RFA alone when using either Radionics (p<0.05) or RITA (p<0.05) equipment (Fig. 3).

Shape of the ablated zone. Comparison of the shape of the cut surface of the ablated zone, as indicated by the ratio of transverse diameter/longitudinal diameter of the ellipsoid, revealed that this ratio tended to be larger with EI-RFA than with RFA using all three types of equipment (Table II). Using Radionics, the ratio was significantly larger with EI-RFA than with RFA using Radionics (p<0.01) (Fig. 4). Thus the ablated zone obtained with RFA became rounder with pretreatment by ethanol injection using Radionics.

The tip temperature after ablation was measured only with Radionics and was not different between RFA and EI-RFA (85.6±9.1 and 85.6±4.1°C, respectively). The ablation times for RFA and EI-RFA using RTC were similar; 293.6±82.8 and 262.7±109.2 sec, respectively.

There was no significant difference in total energy applied between RFA and EI-RFA with Radionics (n=6, 39913.5±10101.1 J and n=6, 35658.5±6620.8 J, respectively). Also, there was no significant difference in total energy between RFA and EI-RFA with RTC (n=7, 13025.7±6190.4 J and n=7, 10041.4±4824.8 J, respectively). More total energy was applied for each ablation session with Radionics compared with RTC for both RFA (p<0.01) and EI-RFA (p<0.01).

There was a significant difference in ablated volume per energy between RFA and EI-RFA using Radionics (n=6, 0.589±0.173 mm³/J and n=6, 1.032±0.345 mm³/J,

Table II. Shape of the ablated area was expressed as the ratio of transverse diameter/longitudinal diameter of the ellipsoid.

Shape (transverse/ longitudinal)	RFA	EI-RFA	p-value
Radionics (n=6)	0.749±0.089	0.955±0.125	0.008[a]
RITA (n=7)	1.089±0.204	1.191±0.171	0.2762
RTC (n=7)	1.346±0.352	1.494±0.393	0.4495

The length of transverse diameter was greater than longitudinal length of EI-RFA compared with that of RFA in all three equipment. [a]Statistically significant (p<0.05).

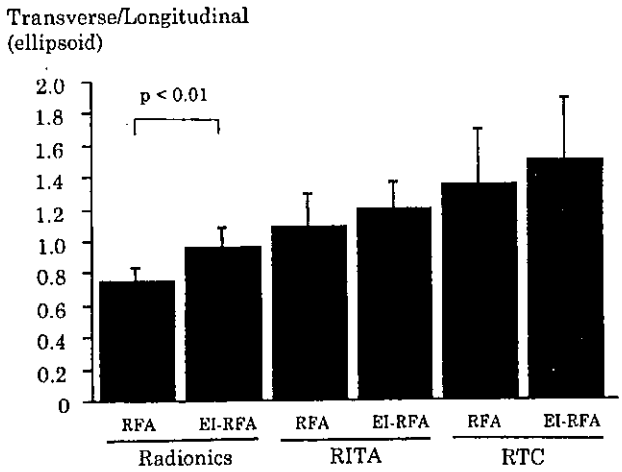

Figure 4. The shape of the ablated area was expressed as the ratio of transverse diameter/longitudinal diameter of the ellipsoid. Using Radionics, a larger ratio was obtained with EI-RFA than with RFA (p=0.0082).

respectively; p<0.05) (Fig. 5), but no significant difference was observed between RFA and EI-RFA using RTC (n=7, 1.729±0.722 mm³/J and n=7, 1.848±1.025 mm³/J, respectively). RTC produced a larger ablation volume per joule with RFA compared with Radionics (p<0.05), but not with EI-RFA.

The number of RFA pulse after setting 130 W power was counted, and no difference was observed between RFA and EI-RFA using Radionics (n=6, 22.8±1.2 and n=6, 23.2±0.8, respectively).

There was a significant difference in ablated volume per current density (ampere/cm²) between RFA and EI-RFA using Radionics (n=6, 3.593±1.294 cm³ and n=6, 5.462± 1.346 cm³, respectively; p<0.05) (Fig. 6).

The ablation times of RFA and EI-RFA were the same, 12 min with Radionics, and 20 min with RITA. The ablation times of RFA and EI-RFA with RTC were 293.6±82.8 sec and 262.7±109.2 sec, respectively. The ablation time was shorter than 5 min for both RFA and EI-RFA using RTC.

Histopathology. The hepatocytes at the center of the ablated zone was deformed with pyknotic nuclei and condensed

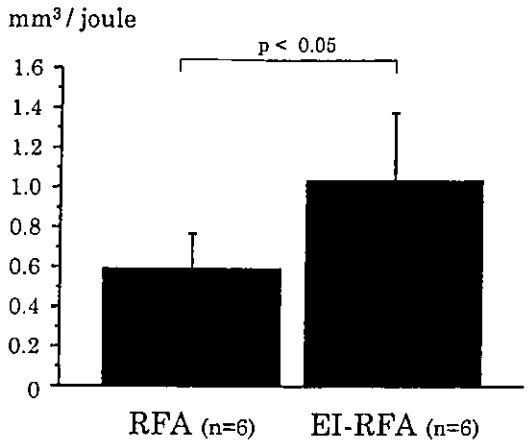

Figure 5. Ablated volume per energy administered with RFA and EI-RFA using Radionics. The ablated volume per energy administered was greater with EI-RFA than with RFA (p=0.0186).

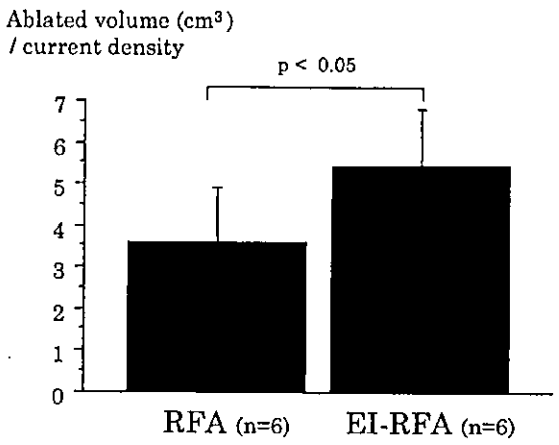

Figure 6. Ablated volume per current density administered with RFA and EI-RFA using Radionics. The ablated volume per current density administered was greater with EI-RFA than with RFA (p=0.0342).

eosinophilic filamentous cytoplasm. At the edge of the ablated zone, there were hyperemic sinusoids and the nuclei and nucleoli of the hepatocytes in the ablated zone showed no apparent differences from those in the viable part of the liver except homogeneous cytoplasm. The loss of stain ability of fragmented red blood cells and the loss of the characteristic shape of the red blood cells due to intravascular hemolysis clearly distinguished the necrotic part from the viable part. Findings of creviced parenchyma formed by splitting of hepatocytes, various-sized round spaces surrounded by compressed hepatocytes, lace-like dilatation of sinusoids, and dilatation of blood vessels were observed similarly in specimens treated by RFA and EI-RFA.

Discussion

RFA has been used to treat liver tumors, and as more cases have been treated, there have been attempts to enlarge the ablation zone by the pretreatment of the ablation area with TAE (9), balloon occlusion of the feeding artery (10,11), and combining RFA with cryosurgical ablation (12). The volume of necrosis was increased by saline-enhanced ablation (13). Also, percutaneous saline-enhanced and impedance-controlled RFA can be effective in the treatment of unresectable hepatic tumors (14). Injection of NaCl before RFA can increase energy deposition, resulting in enlargement of the coagulation size in an animal model with cooled-tip electrodes. Two mechanisms have been proposed to account for the improved tissue heating and increased radiofrequency-induced coagulation with pretreatment by NaCl: a) that NaCl alters tissue properties such as electrical conductivity to permit greater radiofrequency energy deposition, or b) that the infusion of fluid during radiofrequency application improves the thermal conduction within the tissues by causing more rapid and effective convection of heat over a larger tissue volume (15). In addition to these effects, 99.5% ethanol has a strong tissue-dehydration effect, resulting in coagulation necrosis. A radiofrequency lesion is produced by tissue electrocoagulation around the electrode (16). Previous reports indicated that the necrotic zone of liver tumors enlarged by hot ethanol injection compared with cold ethanol injection (17). Regarding the finding that the ablated volume per current density administered was increased by adding ethanol injection using Radionics, the reason for the enlargement of the ablation zone with EI-RFA might be a synergic effect of RFA and heated ethanol.

The standardized RFA settings of each type of equipment almost optimized for treating a liver tumor with a diameter of 3 cm were used for this series of experiments. A preliminary clinical report showed that the EI-RFA technique applied to HCC successfully enlarged the ablation zone (18,19). To apply an enhancing effect of ethanol on RFA is beneficial because an increased number of radiofrequency sessions were related to a higher rate of major complications, such as peritoneal hemorrhage, neoplastic seeding, intrahepatic abscesses, and intestinal perforation (20). The present study showed that EI-RFA augmented the ablation zone 1.52 times with Radionics and 1.56 times with RITA. The sphericity of the ablated zone is ideal for covering spherical lesion. The transverse/longitudinal ratio of the ablated zone significantly increased and sphericity of the zone became increased with ethanol injection using Radionics.

It is not clearly understood why the ethanol injection does not enlarge the ablated zone with RTC. A supplemental effect by ethanol injection to RFA has caused the early roll-off. It might be the characteristics of making current density of the RTC system. Lower boiling point of the injected ethanol (78°C) may cause early impedance rises (roll-off). Complete ablation of the liver tissue is achieved when the tissue desiccation results in an order-of-magnitude increase in the tissue impedance in RTC (21). This prohibits the passage of additional radiofrequency current from the generator. As indicated in the instructions for use of RTC, if roll-off occurs too quickly (<5 min), it indicates that the heating rate may have been too rapid and an undersized thermal lesion may result. In the present experiments, the ablation time was <5 min for both RFA and EI-RFA with RTC.

An *in vivo* experimental study using rabbits showed that the average maximum RFA lesion size increased with

reduced organ perfusion, and that this effect could be accurately monitored using magnetic resonance imaging (22). Also, these authors showed that the major factor influencing the size of the coagulation area is the portal venous flow, and that ligation of the hepatic artery alone does not significantly increase lesion size.

The present study demonstrated that the size of the ablation zone induced was increased by EI-RFA as compared to RFA alone, but no specific pathologic findings associated with EI-RFA were observed. The pathologic changes at the center of the ablated zone clearly included pyknosis of the nuclei and deformity of the cytoplasm of hepatocytes, but the hepatocytes and stromal cells at the edge of the ablated zone apparently remained the same as those in the viable part. In such areas, the presence of fragmented ghost red blood cells in blood vessels and sinusoids due to heat ablation clearly distinguished necrotic parts from viable parts. Ablated specimens do not show necrosis of the hepatocytes, and the structures of sinusoids and liver cell cords remain apparently intact as seen with hematoxylin-eosin staining immediately after RFA, but electron microscopic examination shows irreversible destruction of hepatocyte organelles (23). Scudamore *et al* (24) visualized the necrotic area by staining the tissue for tissue oxidative enzymes using nicotinamide adenine dinucleotide (Sigma Diagnostics) stain to determine if there was evidence of viable tumor within the zone of ablation. This staining method showed loss of enzyme activity that corresponded exactly to the grossly observed ablation zone.

In summary, EI-RFA increased the size of the tissue ablation zone about 1.5 times compared with RFA application alone in fresh bovine liver with Radionics and RITA equipment. The ablated volume per administered energy and the volume per current density were increased by adding ethanol injection to RFA using Radionics. For a given amount of total energy administered, better size and shape of the ablated zone are achieved with EI-RFA than with RFA alone using Radionics and RITA equipment. Based on these findings, the application of concurrent ethanol injection together with RFA is expected to provide a therapeutic choice for localized hepatic tumors.

References

1. Nagata Y, Hiraoka M, Akuta K, Abe M, Takahashi M, Jo S, Nishimura Y, Masunaga S, Fukuda M and Imura H: Radiofrequency thermotherapy for malignant liver tumors. Cancer 65: 1730-1736, 1990.
2. Goldberg SN, Gazelle GS, Solbiati L, Livraghi T, Tanabe KK, Hahn PF and Mueller PR: Ablation of liver tumors using percutaneous RF therapy. Am J Roentgenol 170: 1023-1028, 1998.
3. Allgaier HP, Deibert P, Zuber I, Olschewski M and Blum HE: Percutaneous radiofrequency interstitial thermal ablation of small hepatocellular carcinoma. Lancet 353: 1676-1677, 1999.
4. Curley SA, Izzo F, Ellis LM, Nicolas Vauthey J and Vallone P: Radiofrequency ablation of hepatocellular cancer in 110 patients with cirrhosis. Ann Surg 232: 381-391, 2000.
5. Solbiati L, Livraghi T, Goldberg SN, Ierace T, Meloni F, Dellanoce M, Cova L, Halpern EF and Gazelle GS: Percutaneous radio-frequency ablation of hepatic metastases from colorectal cancer: long-term results in 117 patients. Radiology 221: 159-166, 2001.
6. Livraghi T, Solbiati L, Meloni F, Ierace T, Goldberg SN and Gazelle GS: Percutaneous radiofrequency ablation of liver metastases in potential candidates for resection: the 'test-of-time approach'. Cancer 97: 3027-3035, 2003.
7. Shiina S, Tagawa K, Niwa Y, Unuma T, Komatsu Y, Yoshiura K, Hamada E, Takahashi M, Shiratori Y, Terano A, Omata M, Kawauchi N and Inoue H: Percutaneous ethanol injection therapy for hepatocellular carcinoma: results in 146 patients. Am J Roentgenol 160: 1023-1028, 1993.
8. Goldberg SN, Kruskal JB, Oliver BS, Clouse ME and Gazelle GS: Percutaneous tumor ablation: increased coagulation by combining radio-frequency ablation and ethanol instillation in a rat breast tumor model. Radiology 217: 827-831, 2000.
9. Buscarini L, Buscarini E, Di Stasi M, Quaretti P and Zangrandi A: Percutaneous radiofrequency thermal ablation combined with transcatheter arterial embolization in the treatment of large hepatocellular carcinoma. Ultraschall Med 20: 47-53, 1999.
10. Goldberg SN, Hahn PF, Tanabe KK, Mueller PR, Schima W, Athanasoulis CA, Compton CC, Solbiati L and Gazelle GS: Percutaneous radiofrequency tissue ablation: does perfusion-mediated tissue cooling limit coagulation necrosis? J Vasc Interv Radiol 9: 101-111, 1998.
11. Yamasaki T, Kurokawa F, Shirahashi H, Kusano N, Hironaka K and Okita K: Percutaneous radiofrequency ablation therapy for patients with hepatocellular carcinoma during occlusion of hepatic blood flow. Comparison with standard percutaneous radiofrequency ablation therapy. Cancer 95: 2353-2360, 2002.
12. Bilchik AJ, Wood TF, Allegra D, Tsioulias GJ, Chung M, Rose DM, Ramming KP and Morton DL: Cryosurgical ablation and radiofrequency ablation for unresectable hepatic malignant neoplasms: a proposed algorithm. Arch Surg 135: 657-662, 2000.
13. Livraghi T, Goldberg SN, Monti F, Bizzini A, Lazzaroni S, Meloni F, Pellicano S, Solbiati L and Gazelle GS: Saline-enhanced radio-frequency tissue ablation in the treatment of liver metastases. Radiology 202: 205-210, 1997.
14. Kettenbach J, Kostler W, Rucklinger E, Gustorff B, Hupfl M, Wolf F, Peer K, Weigner M, Lammer J, Muller W and Goldberg SN: Percutaneous saline-enhanced radiofrequency ablation of unresectable hepatic tumors: initial experience in 26 patients. Am J Roentgenol 180: 1537-1545, 2003.
15. Goldberg SN, Ahmed M, Gazelle GS, Kruskal JB, Huertas JC, Halpern EF, Oliver BS and Lenkinski RE: Radio-frequency thermal ablation with NaCl solution injection: effect of electrical conductivity on tissue heating and coagulation-phantom and porcine liver study. Radiology 219: 157-165, 2001.
16. Organ LW: Electrophysiologic principles of radiofrequency lesion making. Appl Neurophysiol 39: 69-76, 1976.
17. Honda N, Guo Q, Uchida H, Ohishi H and Hiasa Y: Percutaneous hot saline injection therapy for hepatic tumors: an alternative to percutaneous ethanol injection therapy. Radiology 190: 53-57, 1994.
18. Kurokohchi K, Watanabe S, Masaki T, Hosomi N, Funaki T, Arima K, Yoshida S, Nakai S, Murota M, Miyauchi Y and Kuriyama S: Combination therapy of percutaneous ethanol injection and radiofrequency ablation against hepatocellular carcinomas difficult to treat. Int J Oncol 21: 611-615, 2002.
19. Kurokohchi K, Watanabe S, Masaki T, Hosomi N, Funaki T, Arima K, Yoshida S, Miyauchi Y and Kuriyama S: Combined use of percutaneous ethanol injection and radiofrequency ablation for the effective treatment of hepatocellular carcinoma. Int J Oncol 21: 841-846, 2002.
20. Livraghi T, Solbiati L, Meloni MF, Gazelle GS, Halpern EF and Goldberg SN: Treatment of focal liver tumors with percutaneous radio-frequency ablation: complications encountered in a multicenter study. Radiology 226: 441-451, 2003.
21. Lin SM, Lin CJ, Chung HJ, Hsu CW and Peng CY: Power rolloff during interactive radiofrequency ablation can enhance necrosis when treating hepatocellular carcinoma. Am J Roentgenol 180: 151-157, 2003.
22. Aschoff AJ, Merkle EM, Wong V, Zhang Q, Mendez MM, Duerk JL and Lewin JS: How does alteration of hepatic blood flow affect liver perfusion and radiofrequency-induced thermal lesion size in rabbit liver? J Magn Reson Imaging 13: 57-63, 2001.
23. Kuromatsu R, Tanaka M, Shimauchi Y, Harada R, Ando E, Itano S, Kumashiro R, Fukuda S, Okuda K and Sata M: Light and electron microscopic analyses of immediate and late tissue damage caused by radiofrequency ablation in porcine liver. Int J Mol Med 11: 199-204, 2003.
24. Scudamore CH, Lee SI, Patterson EJ, Buczkowski AK, July LV, Chung SW, Buckley AR, Ho SG and Owen DA: Radiofrequency ablation followed by resection of malignant liver tumors. Am J Surg 177: 411-417, 1999.

Identification of p46 Shc expressed in the nuclei of hepatocytes with high proliferating activity: Study of regenerating rat liver

JIN YUJI[1], TSUTOMU MASAKI[1], SHUHEI YOSHIDA[1], YUKO KITA[1], HAN FENG[1], NAOHITO UCHIDA[1], HITOSHI YOSHIJI[3], AKIRA KITANAKA[2], SEISHIRO WATANABE[1], KAZUTAKA KUROKOHCHI[1] and SHIGEKI KURIYAMA[1]

[1]Third Department of Internal Medicine and [2]First Department of Internal Medicine, Kagawa University School of Medicine, 1750-1 Ikenobe, Miki-cho, Kita-gun, Kagawa 761-0793; [3]Third Department of Internal Medicine, Nara Medical University, 840 Shijo-cho, Kashihara, Nara 634-8522, Japan

Received December 10, 2003; Accepted February 4, 2004

Abstract. The adaptor molecule Shc is a proto-oncogene product, and it is known to be associated with cell proliferation. However, the role of Shc in the proliferation and regeneration of hepatocytes remains unknown. In the present study, we report that p46 Shc is specifically expressed in the nuclei of proliferative (or regenerative) hepatocytes, suggesting that p46 Shc protein plays a role in hepatocellular proliferation. The expression of Shc was analyzed in liver tissue after partial hepatectomy (PH) or sham operation in Wistar rats by using immunohistochemistry and/or Western blot analysis. In addition, the expression of various cell cycle-related proteins, such as Cdk4, cyclin D1, PCNA, and Cdk1 was analyzed in the tissues of regenerating rat liver. Furthermore, the tyrosine phosphorylation of Shc was studied in liver tissue after PH or sham operation by immunoprecipitation using a monoclonal phosphotyrosine antibody. Although the protein levels of p52 Shc were unchanged in liver tissues after PH or sham operation, tyrosine phosphorylation was detected only in the regenerating rat liver after PH. The levels of p46 Shc protein were markedly increased in liver tissues during the liver regenerative process. In contrast, p66 Shc was not detected in the liver tissues after PH or sham operation. Western blotting and immunohistochemistry showed that the main location of p46 Shc was in the nuclei of proliferating hepatocytes after PH. These data suggest that p46 Shc expressed in hepatocellular nuclei may be closely related to the proliferation of hepatocytes. Therefore, it is suggested that p46 Shc expressed in hepatocellular nuclei may be a useful marker for detecting hepatocytes with high proliferative activity.

Correspondence to: Dr Shigeki Kuriyama, Third Department of Internal Medicine, Kagawa University School of Medicine, 1750-1 Ikenobe, Miki-Cho, Kita-gun, Kagawa 761-0793, Japan
E-mail: skuriyam@kms.ac.jp

Key words: Shc, liver regeneration, cell cycle, proliferation

Introduction

The most established experimental model for studying liver growth control *in vivo* is 70% partial hepatectomy (PH) in rodents, in which most of the remaining hepatocytes synchronously enter the cell cycle and liver mass is restored within 1 to 2 weeks (1). The process of liver regeneration is at least in part controlled by various growth factors and their receptor tyrosine kinases (2-4). For instance, extracellular signal molecules, growth factors that are known to be involved in liver regeneration, include fibroblast growth factor (FGF), (5) platelet-derived growth factor (PDGF) (6), epidermal growth factor (EGF) (7,8), hepatocyte growth factor (HGF) (7,9), and insulin growth factor (IGF) (10). The extracellular signals that trigger regeneration after PH have recently been extensively studied (2-4), but little is known about the intracellular processes of these extracellular signal molecules that regulate the cell cycle control of hepatocytes (11-17).

Many growth factors, cytokines, and adhesion molecules exert their effects by activating specific tyrosine kinesis. The activated receptor allows the docking of additional src homology 2 (SH2) and protein tyrosine binding (PTB) domain-containing adaptor molecules which both coordinate and integrate intracellular signaling events. Src homology and collagen (Shc) is also an SH2-containing cytoplasmic adaptor protein that undergoes phosphorylation by receptors of the tyrosine kinase family, suggesting the possible role of Shc in the proliferative process. The Shc locus is highly conserved throughout evolution, and this locus codes for three overlapping proteins of 66, 52, and 46 kDa (p46 Shc, p52 Shc, and p66 Shc, respectively) (18,19). The p46 Shc and p52 Shc arise from the use of alternative translation initiation sites within the same transcript. In contrast, p66 Shc contains a unique N-terminal region and is generated as a result of an alternative splicing (20). Each isoform can serve as a substrate for activated cytoplasmic or receptor tyrosine

kinases via either the PTB or SH2 domain, and these isoforms can then associate with other SH2 domains containing signal molecules, such as growth receptor-bound 2 (Grb2), an adaptor protein for the Ras exchange factor, son of sevenless (SOS) (21,22). These complexes (p46 Shc/p52Shc-Grb2-SOS) have been shown to activate the Ras-mitogen-activated protein kinase (MAPK) pathway involved in cell proliferation (23-27). Like p46 Shc and p52 Shc, p66 Shc becomes tyrosine-phosphorylated upon the activation of growth factor receptors and forms the p66 Shc/Grb2/SOS complex (24). However, p66 Shc does not affect MAPK activity and inhibits c-fos promoter activation, indicating that p66 Shc may not be involved in Ras activation (19,22,23). Thus, the roles of Shc isoforms in cell proliferation are not straightforward and thus remain controversial (19,28,29,30).

Protein phosphorylation catalyzed by the protein tyrosine and serine/threonine kinases has been recognized as a key regulatory event in a variety of cell functions, such as growth, differentiation, and malignant transformation. We previously demonstrated the importance of protein phosphorylation in signal transduction in relation to the proliferation of normal and transformed hepatocytes (16,31-37). Shc is also a cytoplasmic adaptor protein that undergoes phosphorylation by various receptors of the tyrosine kinase family, including FGF (38), PDGF (39), EGF (18), HGF (7,9,40), and IGF (41) receptors. Therefore, it remains important to study of the role of Shc in the proliferation of hepatocytes; to date, there have been no other studies on this topic. In the present study, we analyzed the levels of p46 Shc, p52 Shc, and p66 Shc as well as their localization in regenerating rat liver. In addition, we examined the relationship between the expression of Shc and cell cycle-related proteins such as cyclin D1, cyclin-dependent kinase 4 (Cdk4), proliferating cellular nuclear antigen (PCNA), and Cdk1, which are present only in the nuclei of proliferating cells. Here, we report that p46 Shc was specifically expressed in the nuclei of the hepatocytes with high proliferative activity during liver regeneration after PH. This report is the first study demonstrating that the main localization of p46 Shc is in the nuclei of highly proliferative hepatocytes.

Materials and methods

Animals. Inbred Wistar rats were bred under specific pathogen-free conditions at the Institute for Animal Experimentation of the Kagawa University School of Medicine. Fifty-five male Wistar rats (8 weeks postnatal; body weight 250-280 g) were used for the present study.

Experimental design. To study the involvement of Shc in liver regeneration, we performed PH on male Wistar rats according to the procedure of Higgins and Anderson (1). Surgery was carried out under ether anesthesia. To analyze the amount of Shc in regenerating rat liver, nuclear and cytosolic fractions as well as whole tissue lysates prepared from liver tissues extracted in 12, 24, 48, 72, and 168 h after PH or sham operation were subjected to Western blot analysis. The localization of Shc was studied by immunohistochemistry using paraffin sections obtained from liver tissues extracted in 12, 24, 48, 72, and 168 h after PH or sham operation. Expression of Shc in the liver tissues of non-treated control rats was also studied by immunohistochemical analysis and Western blot analysis.

Chemicals and antibodies. The avidin-biotin-peroxidase complex (ABC) kit was purchased from Funakoshi Chemical Co., (Tokyo, Japan). All other Chemicals were purchased from Sigma Chemical Co. (Tokyo, Japan) or Wako Pure Chemical Co. (Tokyo, Japan). Two of the anti-Shc antibodies used in this study were purchased from Santa Cruz Biotechnology (Tokyo, Japan). One of these two antibodies was a monoclonal antibody (PG-797) raised against a glutathione S transferase (GST)-tagged fusion protein sequence corresponding to the SH2 domain (amino acids 366-473) of Shc of human and rat origins. The other antibody was an affinity-purified rabbit polyclonal antibody (C-20) raised against a peptide mapped at the carboxy terminus of Shc of human and rat origins. These antibodies were non-reactive with other SH2 domains. The Shc epitope recognized by PG-797 differed from that recognized by C-20. An anti-phosphotyrosine monoclonal antibody (PY20) was also purchased from Santa Cruz Biotechnology (Tokyo, Japan). This antibody reacted to tyrosine-phosphorylated proteins, but not to serine- or threonine-phosphorylated proteins. Anti-cyclin D1 (HD 11) and anti-α tubulin (TU-02) monoclonal antibodies were also purchased from Santa Cruz Biotechnology. Anti-Cdk4 (clone 97), anti-PCNA (clone 24) and anti-Cdk1 (clone 1) monoclonal antibodies were purchased from BD Transductional Laboratories (Tokyo, Japan). All secondary antibodies were purchased from Amersham Life Science (Tokyo, Japan).

Immunohistochemistry of Shc. We prepared 2-μm-thick sections from formalin-fixed, paraffin-embedded tissue blocks. Sections of the liver specimens were immunohistologically stained by the ABC method (Funakoshi Chemical, Tokyo, Japan), as described in our previous study (16,31,33-37). For the detection of Shc, sections were placed in 10 mM citrate buffer (pH 6.0) and the sections were processed at 95°C for 10 min in a microwave oven (RE-M20 Microwave Processor; Sharp, Osaka, Japan). Sections were deparaffinized in xylene, rehydrated in a graded series of alcohol solutions, and then mixed with a solution containing 0.5% hydrogen peroxide in order to block endogenous peroxidase activity. After washing the sections with phosphate-buffered saline (PBS), they were processed for immunostaining. Primary incubation was performed overnight at 24°C with the monoclonal antibody against Shc (1 μg/ml). As a negative control, non-immune mouse IgG was substituted for the primary antibody. For the signal amplification, the Renaissance tyramide signal amplification (TSA) kit (MEN™ Life Science Products, Boston, USA) was used, as described in our previous report (37). Immunoreactivity products were visualized using diaminobenzidine, and the sections were counterstained with Mayer's hematoxylin. The specificity of each immunostaining was further confirmed by an absorption test. Briefly, the primary antibody was mixed with an excess amount of peptides used for immunization, and this absorption test resulted in negative staining in every sample. Thus, these procedures confirmed the specificity of the immunostaining.

The nuclear labeling index of Shc-positive cells (positive nuclei/total cells counted) was determined by evaluating at least 1000 hepatocytes in regenerated, sham-operated, and non-treated rat liver specimens, as determined by two observers (T. Masaki and J. Yuji).

Tissue lysate. Tissue samples were frozen in dry ice immediately after each animal was sacrificed. The samples were homogenized in a lysis buffer [50 mM N-2 hydroxyethylpiperazine-N'-2-ethanesulfonic acid (HEPES; pH 7.0), 250 mM NaCl, 0.1% Nonidet P-40, 100 mM NaF, 200 mM sodium orthovanadate, 0.5 mM phenylmethylsulfonyl fluoride, and 10 μg/ml aprotinin and the lysates were centrifuged at 29,000 x g for 20 min at 4°C.

Preparation of nuclear fractions from liver tissue. The extraction of nuclear proteins was performed according to methods described in our previous report (37). All steps were carried out at 4°C. Liver tissue samples obtained from regenerated, sham-operated, and non-treated rat livers were homogenized in five volumes of 50 mM Tris-HCl (pH 7.4) containing 0.32 M sucrose, 1 mM ethylene glycol-bis (ß-aminoethyl ether)-N, N, N', N'-tetraacetic acid (EGTA), 3 mM benzamidine, 0.1 μg/ml soybean trypsin inhibitor, 10 μg/ml leupeptin, 25 mM KCl, and 5 mM $MgCl_2$. The homogenate was centrifuged at 600 x g for 10 min. The pellet was collected and homogenized in two volumes of 2.2 M sucrose containing 3.3 mM $CaCl_2$, 3 mM benzamidine, 0.1 μg/ml soybean trypsin inhibitor, and 10 μg/ml leupeptin. After centrifugation at 4,000 x g for 60 min, the pellet was collected in the same buffer, and subjected to sodium dodecyl sulfate-polyacrylamide gel (SDS-PAGE) and Western blot analyses.

Preparation of cytosolic fractions in liver tissue. All steps were carried out at 4°C. Tissue samples obtained from regenerated, sham operated, and non-treated rat livers were homogenized in two volumes of 50 mM Tris buffer (pH 7.4) containing 1 mM EGTA, 3 mM benzamidine, 0.1 μg/ml soybean trypsin inhibitor, and 10 μg/ml leupeptin. The homogenate was centrifuged at 8,000 x g for 15 min; the supernatant was then collected and centrifuged at 100,000 x g for 60 min. The supernatant was collected in the same buffer, and subjected to SDS-PAGE and Western blot analyses.

Protein assay. The protein concentration was measured by a dye binding protein assay performed according to the Bradford method (42).

Gel electrophoresis and Western blot analyses. SDS-PAGE was performed according to the method of Laemmli (43), and Western blot analysis was performed as described by Towbin *et al* (44), using the optimal dilution of primary antibodies and horseradish peroxidase-linked secondary antibodies. Optimal dilutions of the antibodies used for Western blotting and/or immunohistochemical analyses were as follows: monoclonal antibody PG 797 (anti-Shc), 1:400; monoclonal antibody HD11 (anti-cyclin D1), 1:300; monoclonal antibody 97 (anti-Cdk4), 1:1000; monoclonal antibody 24 (anti-PCNA), 1:1000; monoclonal antibody 1 (anti-Cdk1), 1:1000; monoclonal antibody TU-02 (anti-α tubulin), horseradish peroxidase anti-mouse immunoglobulin G (IgG), 1:2000; and horseradish peroxidase anti-rabbit IgG, 1:2000. Immunoreactive proteins were visualized with an enhanced chemiluminescence detection system (Amersham) on radiograph film. The exposure time for the Western blot analysis of all samples was 30 sec at room temperature.

Immunoprecipitation. Protein-A sepharose Cl-4B was used to preclean 250-μg protein samples. The samples were incubated with anti-phosphotyrosine monoclonal antibody (PY-20) for 24 h at 4°C, and were then incubated with 50 μl of protein-A sepharose Cl-4B (50%, slurry). The samples were washed four times with immunoprecipitation buffer [50 mM HEPES (pH 8.0), 150 mM NaCl, 2.5 mM EGTA, 1 mM dithiothreitol (DTT), and 0.1% Tween-20] containing 10% glycerol, 0.1 mM phenylmethylsulfonyl fluoride (PMSF), 20 U of aprotinin per ml, 10 mM ß-glycerophosphate, 1 mM NaF, and sodium orthovanadate, and the samples were then washed once with 50 mM HEPES (pH 8.0) containing 1 mM DTT. Immunoprecipitates were resolved and subjected to 12.5% SDS-PAGE. Tyrosine-phosphorylated Shc was detected using the Shc polyclonal antibody (C-20).

Densitometry. The density of the immunoreactive band for Shc on the Western blotting was analyzed by densitometric scanning (Quantity One ver. 4.3, Bio-Rad Laboratories, Co., Ltd., Tokyo, Japan).

Statistical analysis. Data are expressed as the means ± SEM. The significance of differences between observations was determined by Scheffe's multiple comparison method (21). Statistical significance was set at $p<0.05$.

Results

Western blot analysis of Shc in tissue lysates during liver regeneration after PH. Western blot analysis of Shc in liver tissues dissected at 12, 24, 48 and 168 h after PH was carried out using the Shc monoclonal antibody (PG-797). In hepatectomized, sham-operated, and non-treated rat livers, two immunoreactive bands were detected with molecular sizes of 46 and 52 kDa, corresponding to p46 Shc and p52 Shc, respectively (Fig. 1A). The p46 Shc band was much stronger at 24, 48, and 72 h after PH. The immunoreactive band for p46 Shc was faint in the liver tissue at all time points after the sham operation, and the intensity of the p46 Shc band was similar to that in non-treated rat liver tissues. The immunoreactive band for p52 Shc did not change in liver tissue at any time after PH and the sham operation, and the p52 Shc protein levels in these tissues were also similar to those in non-treated rat liver tissues. p66 Shc was not detected in any of the liver tissues after PH and sham-operation. The amount of α-tubulin (an internal control for protein loading) was almost the same in each lane (Fig. 1B).

Densitometric analysis of Western blots of p46 Shc and p52 Shc using liver tissue lysates. Densitometric analysis of the immunoreactive band of p46 Shc on Western blot was performed by means of densitometric scanning. The protein level of p46 Shc was markedly increased at 24 h, and reached

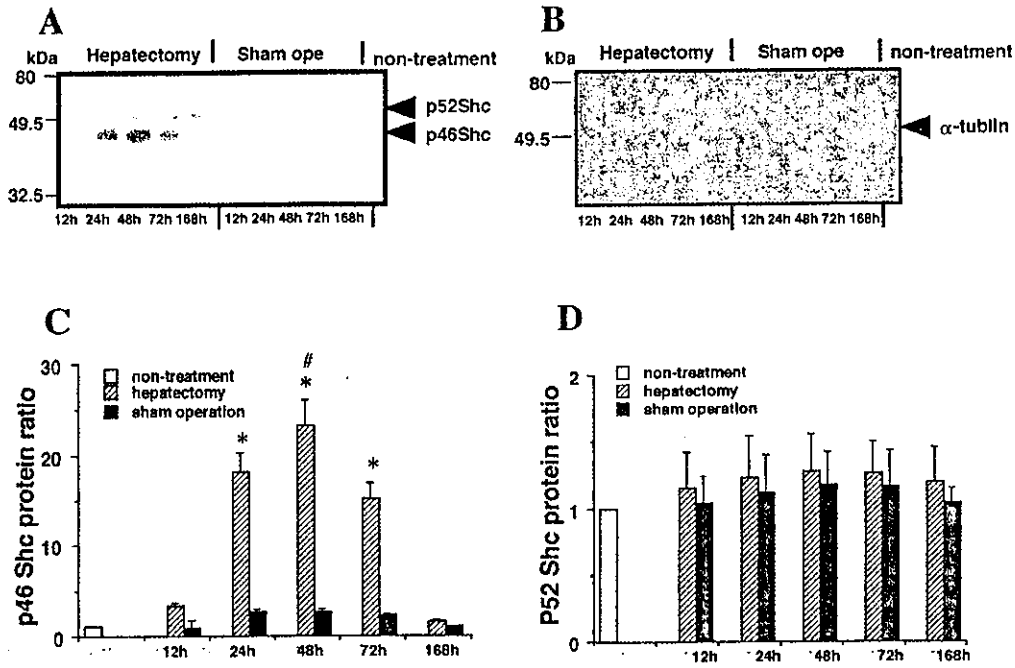

Figure 1. Expression of Shc protein in liver tissues after PH and sham operation. PH and sham operation were performed on male Wistar rats. (A), A total lysate of 50 μg extracted from the liver tissue was subjected to Western blot analysis using Shc monoclonal antibody (PG-797). p46 Shc expression reached maximal levels at 24-72 h after PH. Note that the intensity of the immunoreactive band for p52 Shc did not change in the liver tissues at any time after hepatectomy, sham-operation, and no treatment. (B), The α-tubulin band represents an internal control for the amount of protein loading. Note that the amount of α-tubulin in each lane was identical. (C), Densitometric analysis of the Western blotting of p46 Shc in regenerating rat and sham-operated rat livers. The protein levels in non-treated rat livers were used as a reference level (=1). Values shown represent the mean ± SEM of p46 Shc protein for each group. *p<0.0001 compared with sham-operated rat liver at the corresponding time after operation. #p<0.0001 compared with hepatectomized rat liver at 12, 24, 72, and 168 h after PH. (D), Densitometric analysis of the Western blotting of p52 Shc in the regenerating rat livers and sham-operated rat livers. Note that the expression of p52 Shc did not change during the entire period studied after PH and sham operation.

the maximum level at approximately 48 h after PH (Fig. 1C). Thereafter, the level of p46 Shc gradually decreased to the preoperative level at 168 h after PH (Fig. 1C). The amount of p52 Shc in the liver did not change during the period following the PH and sham operations, in contrast to the amount of p52 Shc in non-treated rat livers (Fig. 1D).

Immunohistochemical analysis of Shc in regenerating rat liver. Although the expression of Shc was almost undetectable in the liver tissues of sham-operated and non-treated rats (control), it was observed in the hepatocellular nuclei of regenerating rat liver, especially 12-72 h after PH (Fig. 2A, arrows). Low levels of Shc were observed in the hepatocellular cytoplasm during the process of liver regeneration. As shown in Fig. 2B, the labeling indexes of Shc-positive hepatocellular nuclei were markedly increased in the liver at 12, 24, 48 and 72 h after PH ($p<0.0001$ as compared with the corresponding sham-operated rat liver, and reached the maximum value at 48 h after PH ($p<0.0001$ as compared with rat liver at 12, 24 and 72 h after PH).

Western blot analysis of Shc expression in nuclear and cytosolic fractions of regenerating liver tissue after PH. To identify the Shc isoforms expressed in the nuclei of hepatocytes during liver regeneration after PH, we performed a Western blot analysis of the expression of Shc isoforms in the nuclear and cytosolic fractions of regenerating rat liver tissue. The expression of Shc was detected as a single band with a molecular size of 46 kDa, which corresponded to p46 Shc in the nuclear fractions of liver tissues dissected after PH in particular 12 hr to 72 h after PH; Fig. 3A). In contrast, p46 Shc expression was not detected in the nuclear fractions of sham-operated and non-treated rat liver tissues. The expression of p52 Shc was detected in the cytosolic fractions of the liver tissues of hepatectomized, sham-operated, and non-treated rats. The amount of p52 Shc remained unchanged in the cytosolic fractions in hepatectomized, sham-operated, and non-treated rat livers. On the other hand, p46 Shc expression was also detected in the cytosolic fractions of the liver tissues removed at 24, 48, and 72 h after PH. p66 Shc was not detected in either the nuclear or in the cytosolic fractions of hepatectomized, sham-operated or non-treated rat livers at the time of examination.

Tyrosine-phosphorylated Shc in regenerating liver tissues after PH. Although the p52 Shc protein levels did not differ between hepatectomized and sham-operated rat livers, tyrosine phosphorylation was detected in the rat liver at 12-168 h after PH, but not in sham-operated and non-treated rat livers (Fig. 4). Furthermore, the p46 Shc expressed in regenerating rat liver was tyrosine-phosphorylated, but that in the sham-operated rat livers was not (Fig. 4).

Western blot analysis of Cdk4, cyclin D1, PCNA, and Cdk1 in liver tissue lysates after PH and sham operation. The expression of Cdk4 (Fig. 5A), cyclin D1 (Fig. 5B), and

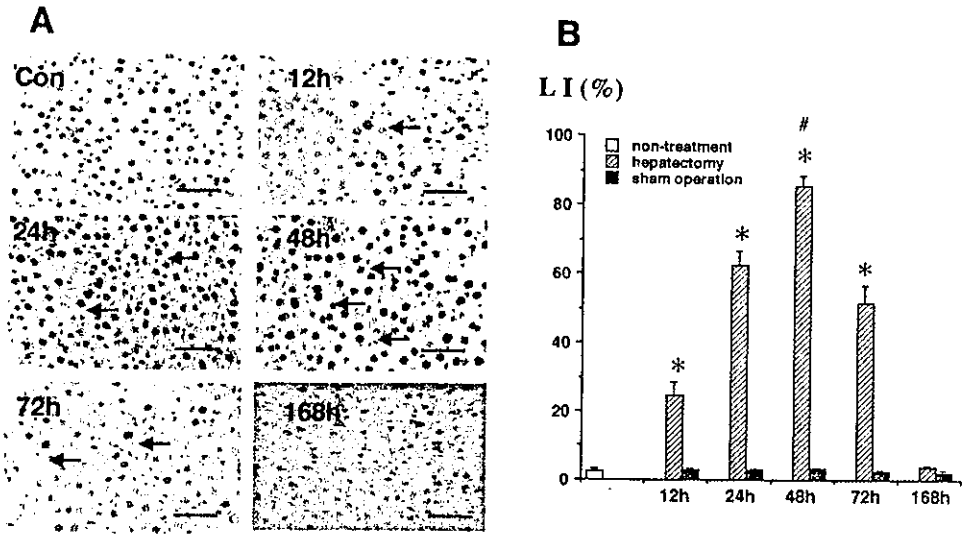

Figure 2. (A), Immunohistological localization of Shc in the liver tissues at 12, 24, 48, 72, and 168 h after PH, and in non-treated rat livers. The expression of Shc was detected in the hepatocellular nuclei in liver tissues at 12, 24, 48, and 72 h after PH (arrows). Bars, 50 μm. (B), Nuclear labeling index for Shc in the liver tissues after PH and sham operation. The labeling index of Shc-positive nuclei of hepatocytes in the liver tissues at 12, 24, 48, and 72 h after PH was significantly higher than that in sham-operated rat liver tissues at the corresponding time after operation (*p<0.0001). The labeling index of Shc reached significantly maximal levels in the liver tissues at 48 h after PH. Values shown represent the mean ± SEM for each group. *p<0.0001 compared with sham-operated rat liver. #p<0.0001 compared with 12, 24, 72, and 168 h after PH.

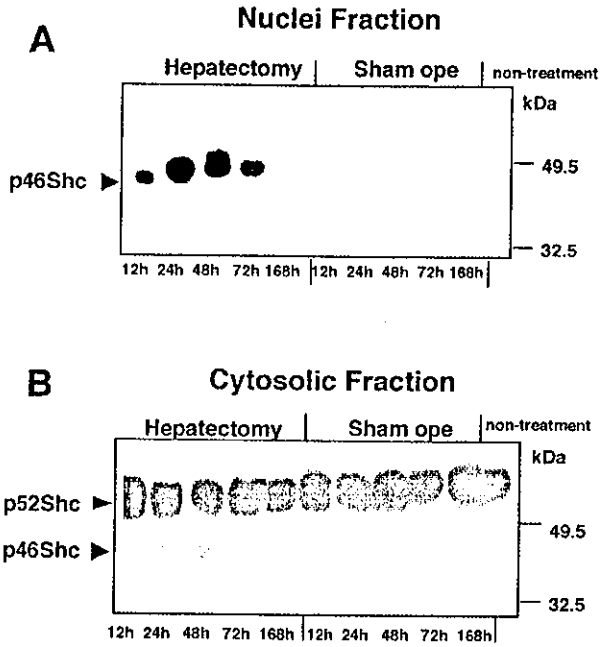

Figure 3. Expression of Shc in the nuclear and cytosolic fractions of liver tissues after PH and sham operation. (A), Western blotting of Shc in the nuclear fractions of liver tissues after PH and sham operation. p46 Shc was detected in the liver tissues from 12 h to 72 h after PH, whereas it was not detected in the liver tissues in the period following the sham operation, nor was it detected in the non-treated rat livers. Other Shc isoforms, i.e., p52 Shc and p66 Shc, were not detected in the nuclear fractions of liver tissues after PH and sham operation. (B), Western blot analysis of Shc in the cytosolic fractions of liver tissues after PH and sham operation. The major isoform of Shc in the cytosolic fractions of hepatectomized, sham-operated and non-treated rat livers was p52 Shc. The p46 Shc was also weakly expressed in liver tissues from 12 to 72 h after PH. The p52 Shc expression in the cytosolic fractions remained unchanged in the liver tissues during the period following PH and the sham operation. The p66 Shc was not detected in the cytosolic fractions of hepatectomized, sham-operated, and non-treated rat livers.

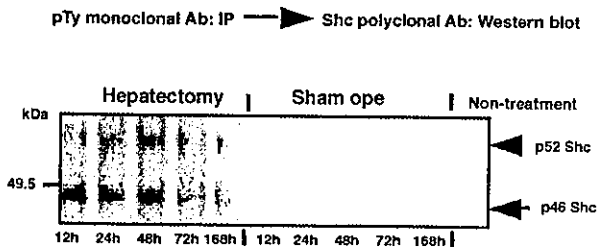

Figure 4. Detection of tyrosine-phosphorylated Shc in the liver tissues after PH and sham operation. Although the levels of p52 Shc did not change in the liver tissues after PH and sham operation (Figs. 1A and 3B), tyrosine-phosphorylated p52 Shc was upregulated in the liver tissues from 12 to 72 h after PH, as compared with that in sham-operated rat livers at the corresponding time (arrow).

PCNA (Fig. 5C) peaked at 24, 48 and 72 h after PH, respectively. The expression of Cdk1 (Fig. 5D) peaked at 48 and 72 h after PH. Very low levels of Cdk4, cyclin D1, PCNA, and Cdk1 were observed in the time course studied following the sham operation (Fig. 5A-D). The expression of these molecules was also very low or undetectable in the non-treated rat liver.

Immunohistochemical analyses of Cdk 4, cyclin D1, PCNA, and Cdk1 in regenerating rat liver after PH. Although the expression of Cdk4, cyclin D1, PCNA, and Cdk1 was almost undetectable in the liver tissues of sham-operated and non-treated rats (data not shown) by immunohistochemistry, the expression of these cell cycle-related molecules was detected in the hepatocellular nuclei of regenerating rat liver after PH (Fig. 5E). The labeling indexes of Cdk4 (Fig. 5F), cyclin D1 (Fig. 5G), PCNA (Fig. 5H), and Cdk1 (Fig. 5I)

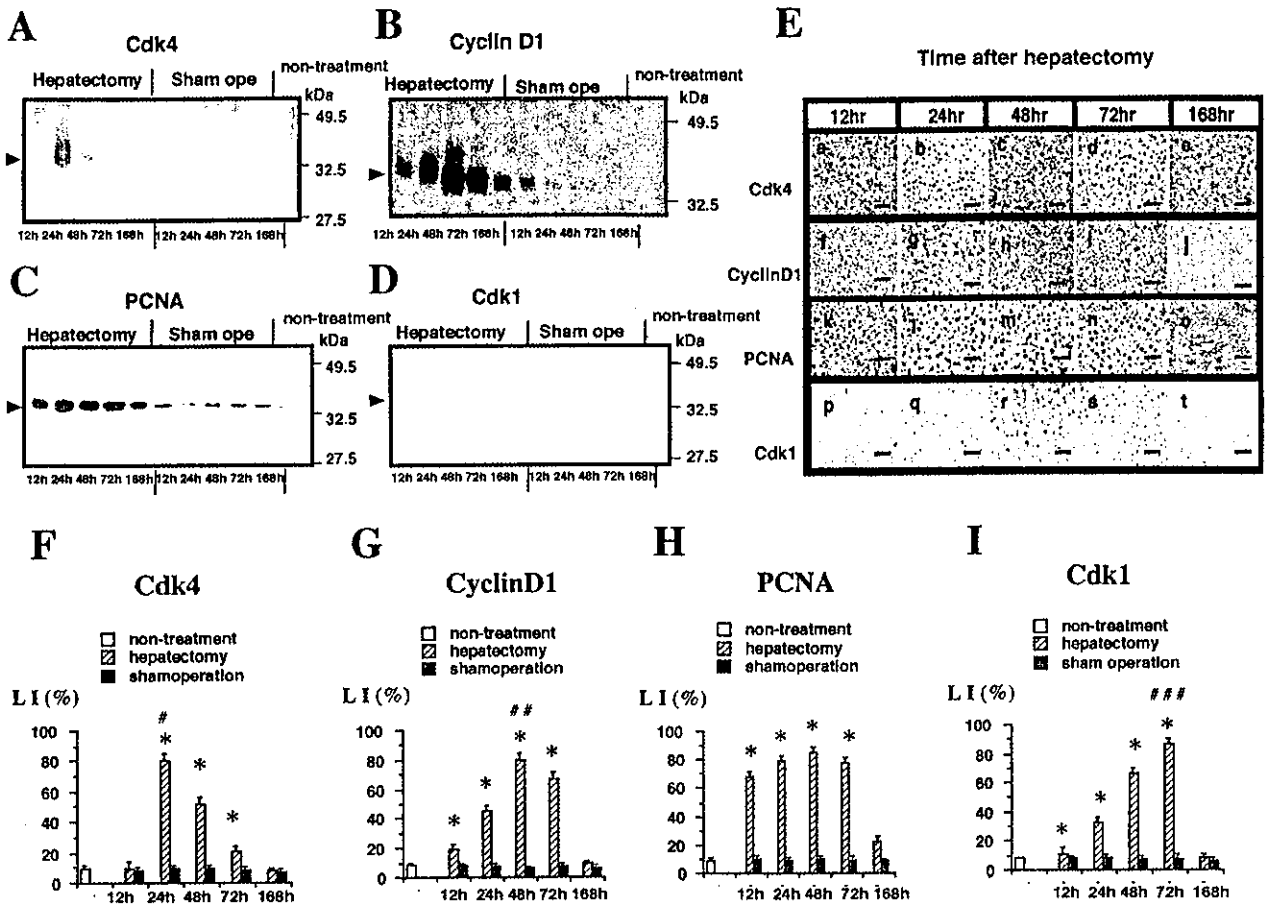

Figure 5. Expression of Cdk4 (A), cyclin D1 (B), PCNA (C), and Cdk1 (D) in the lysate fractions of the liver tissues after PH and sham operation. Note that bands for Cdk4, cyclin D1, PCNA, and Cdk1 were detected in hepatectomized liver tissues, with a peak between 24 and 72 h after PH. The expression of Cdk4, cyclin D1, PCNA, and Cdk1 was very low in sham-operated and non-treated rat liver tissues. (E), Immunohistochemical study of Cdk4 (a-e), cyclin D1 (f-j), PCNA (k-o), and Cdk1 (p-t) after PH. The photographs of (a, f, k, and p), (b, g, l, and q), (c, h, m, and r), (d, i, n, and s), (e, j, o, and t) are sections at 12, 24, 48, 72, and 168 h after PH, respectively. Note that enhanced expression of Cdk4, cyclin D1, PCNA, and Cdk1 was detected in the hepatocellular nuclei of regenerating rat livers after PH. Bars, 50 μm. (F-I), Labeling index of Cdk4 (F), cyclin D1 (G), PCNA (H), and Cdk1 (I). Values shown represent the mean ± SEM. *p<0.0001 compared with rat livers at the corresponding time after sham operation; #p<0.0001 compared with rat liver at 12, 48, 72, and 168 h after PH; ##p<0.0001 compared with rat livers at 12, 24, 72 and 168 h after PH; ###p<0.001 compared with 12, 24, 48, and 168 h after PH.

are shown in the indicated Fig. 5. The results of the immunohistochemical analyses of Cdk4 (Fig. 5E, a-e), cyclin D1 (Fig. 5E, f-j), PCNA (Fig. 5E, k-o), and Cdk1 (Fig. 5E, p-t) were consistent with the Western blot findings. Based on Fig. 5, Fig. 1A and C, Fig. 2 and Fig. 3A, the pattern of p46 Shc expression during liver regeneration after PH resembled that of various cell cycle-related proteins (i.e., Cdk4, cyclin D1, PCNA, and Cdk1).

Discussion

One of the most thoroughly investigated proliferative signal transduction pathways activated by growth factors is the Ras-MAPK cascade (45). Recently, adaptor proteins such as Shc and Grb2, which couple activated receptor protein tyrosine kinases to downstream effectors, have been identified (18). In particular, Shc is believed to be involved in cellular signal transduction in inflammation (46), differentiation (47,48), proliferation (26,27,49), and carcinogenesis (50). However, there have been no reports focusing on the role of Shc in the process of hepatocyte proliferation. This study is the first report to demonstrate that p46 Shc is expressed in the nuclei of hepatocytes, especially in proliferating hepatocytes.

It is well known that Shc is a cytoplasmic signal transducer involved in the transmission of mitogenic signals from various receptor tyrosine kinases to Ras (29). Therefore, it is believed that the expression of Shc is localized in the cytoplasm of cells (51). In the present study, the major location of p52 Shc was shown to be in the hepatocellular cytoplasm, but not in hepatocellular nuclei. Furthermore, p46 Shc expression was detected in the nuclei in the hepatocytes of regenerating rat liver after PH. However, the level of p52 Shc remained unchanged in the liver regeneration process. In the process of liver regeneration after PH, p46 Shc levels increased and reached a peak from 24 to 48 h after PH. It is known that DNA synthesis in the residual liver after PH reaches a peak within 24 to 48 h, when the maximum amount of p46 Shc was also noted. Wolf and Michalopoulos (52) also reported that the number of PCNA-positive hepatocytes reached a peak at 24 h after PH, then gradually decreased, and this number was reduced to only 3% of labeling index

168 h later, when liver regeneration was almost complete. In the present study, in post-PH regenerating liver, the peak time of DNA synthesis and the time point corresponding to the increase in p46 Shc expressed in the hepatocellular nuclei were almost identical to the time points of peak expression of cell cycle-related proteins such as cyclin D1, Cdk 4, PCNA, and Cdk1. These data suggest that p46 Shc expressed in the hepatocellular nuclei might play a role in liver regeneration. Cattaneo *et al* (49) have shown that p46 Shc is associated strictly with proliferative areas in the brain. They reported that although the expression of p46 Shc was not detected in normal astrocytes, it was observed in glial brain tumors with high proliferative activity (49). Fiorucci *et al* (27) also demonstrated that p46 Shc increased in the regenerative process after distal pancreatectomy. Although the localization of p46 Shc expressed in proliferating cells (including cancer cells) remains unknown following these reports, these previous studies support our findings that p46 Shc is overexpressed in proliferative hepatocytes.

The expression of p46 Shc was detected in the pancreas, spleen, and stomach in normal adult mice, as determined by Western blot analysis, whereas it was not observed in the brain, spinal cord, heart, intestine, kidney, lung, and liver (53). We also showed here that the expression of p46 Shc was not detected in the normal rat liver by means of Western blot and/or immunohistochemical analyses, but it was observed in regenerating rat liver. These observations suggest that the induction of p46 Shc expression is associated with hepatocellular proliferation.

In the present study, the levels of p52 Shc protein remained unchanged during liver regeneration. However, tyrosine phosphorylation of p52 Shc was upregulated within 12-72 h after PH (2-4). These data suggest that the tyrosine phosphorylation of p52 Shc might play a role in the process of liver regeneration. It is well known that a number of growth factor receptors are activated during liver regeneration (2-4). Therefore, the tyrosine phosphorylation of p52 Shc might be caused by the upregulation of these various growth receptor kinases during liver regeneration. Such events (p52 Shc tyrosine phosphorylation) have been shown to take place in pancreatic tissues in the regeneration process after distal pancreatectomy (27). In another study, p52 Shc tyrosine phosphorylation was also detected in the proliferative vascular smooth muscle cells after angiotensin II treatment (26). Collectively, these observations suggest that the tyrosine phosphorylation of p52 Shc might play a role in the proliferation of a broad range of cell types, including hepatocytes.

Until this report, the presence of p46 Shc in the nuclei of cells had not been demonstrated. Although the presence of p46 Shc has now been demonstrated in the nuclei of proliferating hepatocytes, its function in these cells remains unclear. In general, it is known that many nuclear proteins have their own nuclear localization signals (NLSs); it appears possible that a protein without its own NLS could enter the nucleus via co-transport with a protein that does have an NLS. Therefore, we tried to detect NLSs in p46 Shc using PSORTS II (http://psort.nibb.ac.jp/), a computer program created for the prediction of protein localization sites in cells (54). We have found that there are two NLSs in the amino acid sequence of human p46 Shc. One NLS is RRRK, corresponding to the 52-55 amino acid sequence of p46 Shc, and the other is RRKP, corresponding to the 53-56 amino acid sequence. These NLSs in p46 Shc might be among several factors expressed in the nuclei of proliferating hepatocytes. It is also known that these NLSs are located in the common amino acid sequences of p46 Shc, p52 Shc, and p66 Shc. The extra N-terminal amino acids of p52 Shc and p66 Shc might interfere with the translocation of p52 Shc and p66 Shc to the nuclei of proliferating hepatocytes.

In conclusion, the presence of p46 Shc in hepatocellular nuclei might be closely related to the proliferation of hepatocytes after PH. In the future, p46 Shc expressed in hepatocellular nuclei might be a useful marker for detecting hepatocytes with high proliferative activity. Further studies are required to explore this possibility.

Acknowledgments

This study was supported in part by a Grant-in-Aid for Scientific Research (B-14370185 and C-15590654) from the Ministry of Education, Culture, Sports, Science and Technology.

References

1. Higgins GM and Anderson RM: Experimental pathology of liver. I. Restoration of liver of white rat following partial surgical removal. Arch Pathol 12: 186-202, 1931.
2. Michalopoulos GK and De Frances MC: Liver regeneration. Science 276: 60-66, 1997.
3. Fausto N: Liver generation: from laboratory to clinic. Liver Transpl 7: 835-844, 2001.
4. Steer CJ: Liver generation. FASEB J 9: 1396-1400, 1995.
5. Kan M, Huang JS, Mansson PE, Yasumitsu H, Carr B and McKeehan WL: Heparin-binding growth factor type 1 (acidic fibroblast growth factor): a potential biphasic autocrine and paracrine regulator of hepatocyte regeneration. Proc Natl Acad Sci USA 86: 7432-7436, 1989.
6. Kimura M and Ogihara M: Proliferation of adult rat hepatocytes in primary cultures induced by platelet-derived growth factor is potentiated by phenylephrine. Jpn J Pharmacol 76: 165-174, 1998.
7. Fausto N, Laird AD and Webber EM: Liver regeneration. 2. Role of growth factors and cytokines in hepatic regeneration. FASEB J 9: 1527-1536, 1995.
8. Mullhaupt B, Feren A, Fodor E and Jones A: Liver expression of epidermal growth factor RNA. Rapid increases in immediate-early phase of liver regeneration. J Biol Chem 269: 19667-19670, 1994.
9. Adachi T, Nakashima S, Saji S, Nakamura T and Nozawa Y: Roles of prostaglandin production and mitogen-activated .protein kinase activation in hepatocyte growth factor-mediated rat hepatocyte proliferation. Hepatology 21: 1668-1674, 1995.
10. Streck RD and Pintar JE: The embryonic pattern of rat insulin-like growth factor-I gene expression suggests a role in induction and early growth of the liver. Endocrinology 131: 2030-2032, 1992.
11. Jaumot M, Estanyol JM, Serratosa J, Agell N and Bachs O: Activation of cdk4 and cdk2 during rat liver regeneration is associated with intranuclear rearrangements of cyclin-cdk complexes. Hepatology 29: 385-395, 1999.
12. Schwabe RF, Bradham CA, Uehara T, Hatano E, Bennett BL, Schoonhoven R and Brenner DA: c-Jun-N-terminal kinase drives cyclin D1 expression and proliferation during liver regeneration. Hepatology 37: 824-832, 2003.
13. Luedde T, Rodriguez ME, Tacke F, Xiong Y, Brenner DA and Trautwein C: p18(INK4c) collaborates with other CDK-inhibitory proteins in the regenerating liver. Hepatology 37: 833-841, 2003.
14. Rickheim DG, Nelsen CJ, Fassett JT, Timchenko NA, Hansen LK and Albrecht JH: Differential regulation of cyclins D1 and D3 in hepatocyte proliferation. Hepatology 36: 30-38, 2002.

15. Pediaditakis P, Lopez-Talavera JC, Petersen B, Monga SP and Michalopoulos GK: The processing and utilization of hepatocyte growth factor/scatter factor following partial hepatectomy in the rat. Hepatology 34: 688-693, 2001.
16. Masaki T, Tokuda M, Fujimura T, Ohnishi M, Tai Y, Miyamoto K, Itano T, Matsui H, Watanabe S, Sogawa K, Yamada T, Konishi R, Nishoka M and Hatase O: Involvement of annexin I and annexin II in hepatocyte proliferation: can annexins I and II be markers for proliferative hepatocytes? Hepatology 20: 425-435, 1994.
17. Loyer P, Glaise D, Cariou S, Baffet G, Meijer L and Guguen-Guillouzo C: Expression and activation of cdks (1 and 2) and cyclins in the cell cycle progression during liver regeneration. J Biol Chem 269: 2491-2500, 1994.
18. Pelicci G, Lanfrancone L, Grignani F, McGlade J, Cavallo F, Forni G, Nicoletti I, Grignani F, Pawson T and Pelicci PG: A novel transforming protein (SHC) with an SH2 domain is implicated in mitogenic signal transduction. Cell 70: 93-104, 1992.
19. Migliaccio E, Mele S, Salcini AE, Pelicci G, Lai KM, Superti-Furga G, Pawson T, Di Fiore PP, Lanfrancone L and Pelicci PG: Opposite effects of the p52shc/p46shc and p66shc splicing isoforms on the EGF receptor-MAP kinase-fos signalling pathway. EMBO J 16: 706-716, 1997.
20. Luzi L, Confalonieri S, Di Fiore PP and Pelicci PG: Evolution of Shc functions from nematode to human. Curr Opin Genet Dev 10: 668-674, 2000.
21. Salcini AE, McGlade J, Pelicci G, Nicoletti I, Pawson T and Pelicci PG: Formation of Shc-Grb2 complexes is necessary to induce neoplastic transformation by overexpression of Shc proteins. Oncogene 9: 2827-2836, 1994.
22. Lanfrancone L, Pelicci G, Brizzi MF, Aronica MG, Casciari C, Giuli S, Pegoraro L, Pawson T, Pelicci PG and Arouica MG: Overexpression of Shc proteins potentiates the proliferative response to the granulocyte-macrophage colony-stimulating factor and recruitment of Grb2/SoS and Grb2/p140 complexes to the beta receptor subunit. Oncogene 10: 907-917, 1995.
23. Marshall MP: Ras target proteins in eukaryotic cells. FASEB J 9: 1311-1318, 1995.
24. Gotoh N, Toyoda M and Shibuya M: Tyrosine phosphorylation sites at amino acids 239 and 240 of Shc are involved in epidermal growth factor-induced mitogenic signaling that is distinct from Ras/mitogen-activated protein kinase activation. Mol Cell Biol 17: 1824-1831, 1997.
25. Faraldo MM, Deugnier MA, Thiery JP, Glukhova MA, Thiery JP and Glukhova MA: Growth defects induced by perturbation of beta1-integrin function in the mammary gland epithelium result from a lack of MAPK activation via the Shc and Akt pathways. EMBO Rep 2: 431-437, 2001.
26. Sayeski PP and Ali MS: The critical role of c-Src and the Shc/Grb2/ERK2 signaling pathway in angiotensin II-dependent VSMC proliferation. Exp Cell Res 15: 339-349, 2003.
27. Fiorucci S, Bufalari A, Distrutti A, Lanfrancone L, Servoli A, Sarpi L, Federici B, Bartoli A, Morelli A and Moggi L: Bombesin-induced pancreatic regeneration in pigs is mediated by p46Shc/p52Shc and p42/p44 mitogen-activated protein kinase upregulation. Scand J Gastroenterol 33: 1310-1320, 1998.
28. Migliaccio E, Giorgio M, Mele S, Pelicci G, Reboldi P, Pandolfi PP, Lanfrancone L and Pelicci PG: The p66shc adaptor protein controls oxidative stress response and life span in mammals. Nature 402: 309-313, 1999.
29. Bonfini L, Migliaccio E, Pelicci G, Lanfrancone L and Pelicci PG: Not all Shc's roads lead to Ras. Trends Biochem Sci 21: 257-261, 1996.
30. Okada S, Kao AW, Ceresa BP, Blaikie P, Margolis B and Pessin JE: The 66-kDa Shc isoform is a negative regulator of the epidermal growth factor-stimulated mitogen-activated protein kinase pathway. J Biol Chem 272: 28042-28049, 1997.
31. Masaki T, Tokuda M, Ohnishi M, Watanabe S, Fujimura T, Miyamoto K, Itano T, Matsui H, Arima K, Shirai M, Maeba T, Sogawa K, Konishi R, Taniguchi K, Hatanaka Y, Hatase O and Nishioka M: Enhanced expression of the protein kinase substrate annexin I in human hepatocellular carcinoma. Hepatology 24: 72-81, 1996.
32. Masaki T, Okada M, Shiratori Y, Rengifo W, Matsumoto K, Maeda S, Kato N, Kanai F, Komatsu Y, Nishioka M and Omata M: $pp60^{c\text{-}src}$ activation in hepatocellular carcinoma of human and LEC rat. Hepatology 27: 1257-1264, 1998.
33. Masaki T, Okada M, Tokuda M, Shiratori Y, Hatase O, Shirai M, Nishioka M and Omata M: Reduced C-trminal src kinase (Csk) activities in human hepatocellular carcinoma. Hepatology 29: 379-384, 1999.
34. Masaki T, Shiratori Y, Rengifo W, Igarashi K, Hatanaka Y, Nishioka M and Omata M: Hepatocellular carcinoma cell cycle: study of LEC rat. Hepatology 32: 711-720, 2000.
35. Masaki T, Shiratori Y, Rengifo W, Igarashi K, Yamagata M, Kurokochi K, Uchida N, Miyauchi Y, Yoshiji H, Watanabe S, Omata M and Kuriyama S: Cyclins and cyclin-dependent kinases: comparative study of hepatocellular carcinoma versus liver cirrhosis. Hepatology 37: 534-543, 2003.
36. Yamagata M, Masaki T, Okudaira T, Imai Y, Shiina S, Shiratori Y and Omata M: Small hyperechoic nodules in chronic liver diseases include hepatocellular carcinomas with low cyclin D1 and Ki-67 expression. Hepatology 29: 1722-1729, 1999.
37. Masaki T, Tokuda M, Shiratori Y, Shirai M, Matsumoto K, Nishioka M and Omata M: A possible novel src-related tyrosine kinase in cancer cells of LEC rats that develop hepatocellular carcinoma. J Hepatol 32: 92-99, 2000.
38. Vainikka S, Joukov V, Wennstrom S, Bergman M, Pelicci PG and Alitalo K: Signal transduction by fibroblast growth factor receptor-4 (FGFR-4). Comparison with FGFR-1. J Biol Chem 269: 18320-18326, 1994.
39. Yokote K, Mori S, Hansen K, McGlade J, Pawson T, Heldin CH and Claesson-Welsh L: Direct interaction between Shc and the platelet-derived growth factor beta-receptor. J Biol Chem 269: 15337-15343, 1994.
40. Pelicci G, Giordano S, Zhen Z, Salcini AE, Lanfrancone L, Bardelli A, Panayotou G, Waterfield MD, Ponzetto C, Pelicci PG and Comoglio PM: The motogenic and mitogenic responses to HGF are amplified by the Shc adaptor protein. Oncogene 10: 1631-1638, 1995.
41. Pronk GJ, McGlade J, Pelicci G, Pawson T and Bos JL: Insulin-induced phosphorylation of the 46- and 52-kDa Shc protein. J Biol Chem 268: 5748-5753, 1993.
42. Bradford MM: A rapid and sensitive method for the quantitation of microgram quantities of protein utilizing the principle of protein-dye binding. Anal Biochem 72: 248-254, 1976.
43. Laemmli UK: Cleavage of structural proteins during the assembly of the head of bactriophage T4. Nature 227: 680-685, 1970.
44. Towbin H, Stadhelin T and Gordon J: Electrophoretic transfer of proteins from polyacrylamide gel to nitrocellulose sheets: procedure and some applications. Proc Natl Acad Sci USA 76: 4350-4354, 1979.
45. Stork PJ and Schmitt JM: Crosstalk between cAMP and MAP kinase signaling in the regulation of cell proliferation. Trends Cell Biol 12: 258-266, 2002.
46. Bates ME, Busse WW and Bertics PJ: Interleukin 5 signals through Shc and Grb 2 in human eosinophils. Am J Respir Cell Mol Biol 18: 75-83, 1998.
47. Laurino C and Cordera R: Role of IRS-1 and SHC activation in 3T3-L1 fibroblasts differentiation. Growth Horm IGF Res 8: 363-367, 1998.
48. Conti L, Sipione S, Magrassi L, Bonfanti L, Rigamonti D, Pettirossi V, Peschanski M, Haddad B, Pelicci P, Milanesi G, Pelicci G and Cattaneo E: Shc signaling in differentiating neural progenitor cells. Nat Neurosci 4: 576-586, 2001.
49. Cattaneo E and Pelicci PG: Emerging roles for SH2/PTB-containing Shc adaptor proteins in the developing mammalian brain. Trends Neurosci 21: 476-481, 1998.
50. Pelicci G, Lanfrancone L, Salcini AE, Romano A, Male S, Grazia Borrello M, Segatto O, Di Fiore PP and Pelicci PG: Constitutive phosphorylation of Shc proteins in human tumors. Oncogene 11: 899-907, 1995.
51. Clark SF, Martin S, Carozzi AJ, Hill MM and James DE: Intracellular localization of phosphatidylinositide 3-kinase and insulin receptor substrate-1 in adipocytes: potential involvement of a membrane skeleton. J Cell Biol 140: 1211-1225, 1998.
52. Wolf HK and Michalopoulos GK: Hepatocyte regeneration in acute fulminant hepatitis: a study of proliferating cell nuclear antigen expression. Hepatology 15: 707-713, 1992.
53. O'Bryan JP, Songyang Z, Cantley L, Der CJ and Pawson T: A mammalian adaptor protein with conserved Src homology 2 and phosphotyrosine-binding domains is related to Shc and is specifically expressed in the brain. Proc Natl Acad Sci USA 93: 2729-2734, 1996.
54. Nakai K: Protein sorting signals and prediction of subcellular localization. Adv Protein Chem 54: 277-344, 2000.

Percutaneous ethanol and lipiodol injection therapy for hepatocellular carcinoma

KAZUTAKA KUROKOHCHI, TSUTOMU MASAKI, YOSHIAKI MIYAUCHI, TOSHIHARU FUNAKI, HIROHITO YONEYAMA, HISAAKI MIYOSHI, SHUHEI YOSHIDA, TAKASHI HIMOTO, ASAHIRO MORISHITA, NAOHITO UCHIDA, SEISHIRO WATANABE and SHIGEKI KURIYAMA

Third Department of Internal Medicine, Kagawa University School of Medicine, 1750-1 Ikenobe, Miki-cho, Kita-gun, Kagawa 761-0793, Japan

Received September 29, 2003; Accepted November 12, 2003

Abstract. Radiofrequency ablation (RFA) therapy is of great significance in the treatment of hepatocellular carcinoma (HCC) or metastatic liver tumors. RFA is able to achieve widely coagulated necrosis in a few sessions without major complications. However, HCC cases exist that are resistant to RFA therapy for several reasons. In the present study, we performed injection of the mixture of ethanol and lipiodol (percutaneous ethanol-lipiodol injection therapy: PELIT) for HCCs that lacked clear visuality of the entire shape of the tumor by ultrasonography (US) or computed tomography (CT), or that were difficult to treat with RFA alone due to their locations in the liver or due to severe liver dysfunction of the patients. Local recurrence rates of HCC treated with PELIT were shown to be low in patients followed up for at least 4 months. In all patients treated with PELIT, lipiodol was accumulated in the entire region of the tumor after several trials of PELIT and the accumulation was kept for many months. The biopsy examination from the tumor treated with PELIT showed that HCC cells were totally destroyed by the PELIT. Although RFA therapy serves as a central role for the treatment of HCCs, PELIT, considered to be milder therapy, is likely to be important as a supportive treatment for HCCs and useful for the treatment of HCCs that are difficult to treat with RFA.

Introduction

Hepatocellular carcinoma (HCC) is usually formed on the cirrhotic condition of the liver caused by hepatitis B and C virus infection. We have shown that the underlying liver cirrhosis is not only a major obstacle for achieving successful treatment for HCC but also a factor promoting intrahepatic invasion and metastasis of HCC (1-3). Despite the intensive efforts for the development of novel treatment modalities for HCC, the prognosis of HCC remains relatively poor (4,5). The feasibility of gene therapy for HCC has therefore been investigated intensively in animal models using viral and non-viral systems (6-16), since these are important for evaluating new treatment modalities for HCC. Several options for the treatment of HCC are now ongoing, such as percutaneous ethanol injection (PEI), radiofrequency ablation (RFA) and transcatheter arterial injection or embolization (TAI or TAE). Among these treatments, RFA appears to be very effective for inducing coagulated necrosis of HCCs (17-20) or metastatic liver tumors (21,22) without major complications. It is thought that this treatment will serve as a central role for the treatment of HCC from the standpoint of its effectiveness and easiness for handling. Moreover, we have reported that the combined use of PEI and RFA is more effective to achieve the larger coagulated necrosis compared with RFA alone (23,24) and that this combination therapy can be adapted to the HCCs that are difficult to treat with RFA alone (25). PEI-RFA is likely to be attractive especially for the patients with large-sized HCCs. However, in contrast to its effectiveness for inducing widely coagulated necrosis, it is pointed out that the rate of local recurrence of HCC after RFA is likely to be relatively high in the cases under insufficient RFA treatment (26). Moreover, we have to face the HCCs that are difficult to treat with RFA alone because of the lack of clear visuality of the tumor by ultrasonography (US) or computed tomography (CT), the location of the tumor in the liver or severe liver dysfunction of the patients. To overcome these problems, we developed a new treatment modality, namely percutaneous ethanol-lipiodol injection therapy (PELIT), a modified PEI therapy. We performed PELIT against HCCs that were resistant to RFA and evaluated its usefulness for the treatment of HCC.

Subjects and methods

Patients. PELIT was performed in 19 patients (14 males and 5 females; mean age of 65 years) with biopsy-proven HCCs. All the patients were followed up for at least 4 months after the initial PELIT. These cases were considered to be more suitable

Correspondence to: Dr Shigeki Kuriyama, Third Department of Internal Medicine, Kagawa University School of Medicine, 1750-1 Ikenobe, Miki-cho, Kita-gun, Kagawa 761-0793, Japan
E-mail: skuriyam@kms.ac.jp

Key words: percutaneous ethanol-lipiodol injection therapy, hepatocellular carcinoma, hepatic reserve, local treatment, radiofrequency ablation

Table I. Characteristics of patients with HCC treated with PELIT.

Patient no.	Gender	Tumor site	Tumor size (cm)	Observation period (months)	Duration of no local recurrence (months)	Reasons for PELIT
1	F	S5	1.5	7	7	I
2	F	S7	2.0	11	11	R, I, H
2	F	S1	3.0	4	4	R, D
3	M	S7	1.0	15	15	L
4	M	S7	1.5	14	14	I
5	M	S8	1.0	12	12	I, H
6	M	S8	2.5	11	11	I
7	F	S7	1.5	12	12	L
8	F	S6	1.5	8	8	I
9	M	S7	2.0	7	7	R
10	M	S3	2.0	8	8	I, H
11	M	S5	2.5	8	8	I, H
12	M	S4	2.0	7	**6**	I
13	M	S3	2.0	4	4	I
14	M	S8	1.5	7	7	D
15	M	S8	2.0	7	5	D
16	M	S7	1.5	4	4	R
17	F	S4	1.5	15	**13**	I
18	M	S6	1.5	4	4	I
19	F	S5	1.5	11	11	D, R

Characteristics of the patients (20 nodules in 19 patients) treated with PELIT are listed. Although the local recurrence was observed in 2 patients (no. 12 and 17), the recurrent lesions were controllable with additional PELIT. Bold numbers, the cases with local recurrence after PELIT. The reason why PELIT was chosen as a treatment are classified as follows: H, hypovascular HCC; I, HCC invisible by US or CT; D, HCC difficult to treat with RFA; R, HCC with severe hepatic reserve; L, HCC of local recurrence after RFA.

to PELIT than RFA therapy. PELIT was chosen for the treatment of HCCs because these patients had hypovascular HCC (H), or HCC invisible by US or CT (I), or HCC difficult to treat with RFA (D), or HCC with severe hepatic reserve (R), or local recurrence after the initial RFA therapy (L). These reasons are shown in Table I. The representative 5 cases are summarized in the results.

Treatments. PELIT was performed under the real-time US guidance with a 3.5-MHz sector probe (Power Vision 5000; Toshiba Medical, Tokyo, Japan). A 21 gauge fine needle for PEI was inserted into the tumor in the liver, and then the mixture of ethanol (99.5%) and lipiodol (Japan Shering, Osaka, Japan), a lipid-based contrast medium, at a ratio of 10:1, was slowly injected into the tumor. The volume of injected ethanol-lipiodol was always kept below the double volume of the estimated tumor volume. The studies were conducted with informed consent given by all patients at the time of enrollment to this study.

Evaluation of therapeutic efficacy. Five to seven days after PELIT, plain or contrast-enhanced CT was performed to evaluate the response to PELIT. Tumor necrosis was considered to be complete when no foci with early enhancement by the dynamic CT study were seen around the original tumor lesion.

Results

Treatment of PELIT on HCCs. For PELIT, the mixture of 99.5% ethanol and lipiodol at a ratio of 10:1 was used. After mixing the lipiodol with ethanol, the color of the resulting fluid was clear, not milky, indicating that lipid-based lipiodol and ethanol could be mixed well at this ratio. It is noteworthy that the mixture of ethanol and lipiodol became cloudy when kept under the air condition for several hours. Among 19 patients who received PELIT, reversible liver dysfunction with slight elevation of serum levels of transaminase was observed in 2 patients. In these 2 patients, over-flow of the mixture of lipiodol-ethanol outside the tumorous lesion was observed in performing PELIT. In the remaining 17 patients, no adverse reactions were detected after PELIT. Throughout the whole study, the flow and the pooling of the mixture of ethanol-lipiodol were more clearly visible by US during the injection into the tumors, compared with the cases injected with ethanol without lipiodol. The results of 19 patients who were followed up for at least 4 months after the first PELIT are summarized in Table I. Most of the HCCs treated were <3 cm in diameter except a tumor of patient no. 2. For this patient with HCC that was 3 cm in diameter, PELIT was chosen, because the HCC was located in the S1 region in the liver and the approach route of an RFA electrode was

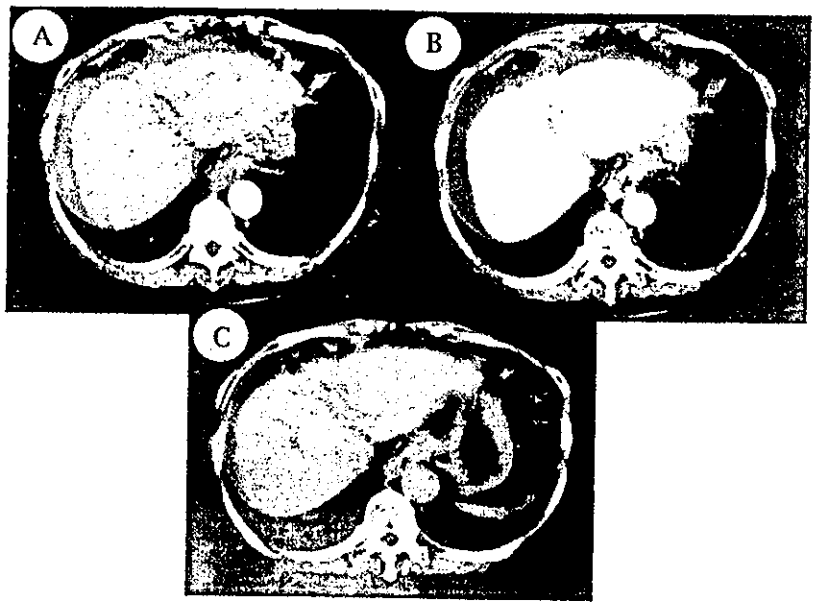

Figure 1. Contrast-enhanced CT before (A, early phase; B, late phase) and immediately after PELIT (C) for HCC (2 cm) located in the S5 region of the liver. The HCC was located close to the main tract and the umbilical portion of the portal vein, which made it difficult to insert an RFA electrode into the tumor. Furthermore, the hepatic reserve of the patient was not sufficient for RFA therapy. After PELIT, lipiodol was observed in the entire lesion of the tumor.

prevented by the gallbladder and the portal tract. Furthermore, liver dysfunction was very severe in this patient. Only in 2 of 20 nodules in 19 patients, local recurrence was detected at the period shown (Table I). In patients no. 4 and 7, locally recurring HCCs after RFA were treated with PELIT and no new recurrence has been detected for over a year. Fig. 1 shows the contrast-enhanced CT before (A and B) and immediately after PELIT (C) for HCC located in the S5 region of the liver in patient no. 19. In this case, the tumor was a typical HCC, showing the enhancement in the early phase and defect in the late phase of the dynamic CT. The tumor was located close to the portal tract and seemed to be difficult to treat with RFA. Moreover, the liver dysfunction of this patient was too severe to undergo RFA therapy. The mixture of ethanol-lipiodol was injected into the tumor using a PEIT needle. Immediately after the PELIT, the mixture of ethanol-lipiodol was accumulated in the entire region of the tumor. To confirm that all the cancer cells in the region of lipiodol-deposit were destroyed, liver biopsy of lipiodol-accumulated region was performed. The biopsy specimen showed the nuclei of all HCC cells had disappeared and the whole tumor was destroyed by PELIT, although the accumulation of lipiodol was not microscopically observed in the specimen (Fig. 2).

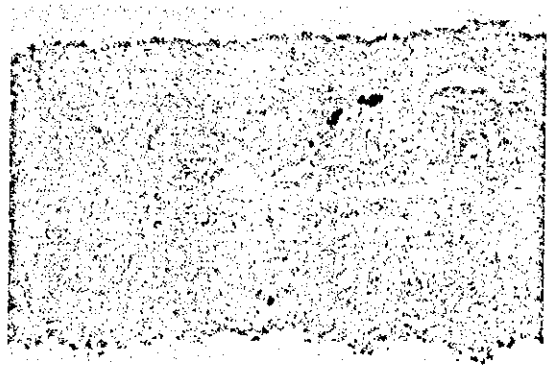

Figure 2. Liver biopsy specimen obtained from the tumor treated with PELIT. Liver biopsy specimen obtained from the HCC in the S5 region of the liver shown in Fig. 1 after the PELIT revealed that the nuclei of all cells had disappeared and the HCC cells were necrotic. Hematoxylin and eosin staining. Magnification x100.

Effects of PELIT on HCC invisible by US or CT. Fig. 3 represents the US (A), and the CT before (B) and immediately after (C) the PELIT for HCC located in the S8 region of the liver in patient no. 6. The size of the HCC was 2.5 cm in diameter. In this patient, the location of the tumor was not visible by US as shown (Fig. 3A), although it was clearly visible by CT (Fig. 3B). PELIT was performed under the US guidance, based on the CT finding, and 12 ml of mixture of ethanol-lipiodol was injected into the tumor. The mixture of ethanol-lipiodol was accumulated in the entire region of the tumor after PELIT (Fig. 3C). The dynamic CT taken 10 months after PELIT also showed the good retention of accumulated lipiodol and no enhancement around the tumor in the early phase (data not shown). PELIT was performed for another patient (no. 5) with HCC not visible by US. In this patient, the HCC located in the S8 region immediately under the diaphragm (Fig. 4A) was not visible by US, and to make matters worse, the degree of liver dysfunction was too severe to undergo RFA therapy. The accumulation of lipiodol-ethanol reached beyond the margin of the tumorous lesion in this case (Fig. 4B).

Effects of PELIT on HCC difficult to treat with RFA and with severe hepatic reserve. Fig. 5 shows HCC located in the S7 region in the liver before (A and B) and after (C) the first PELIT. Liver dysfunction of this patient was also very severe,

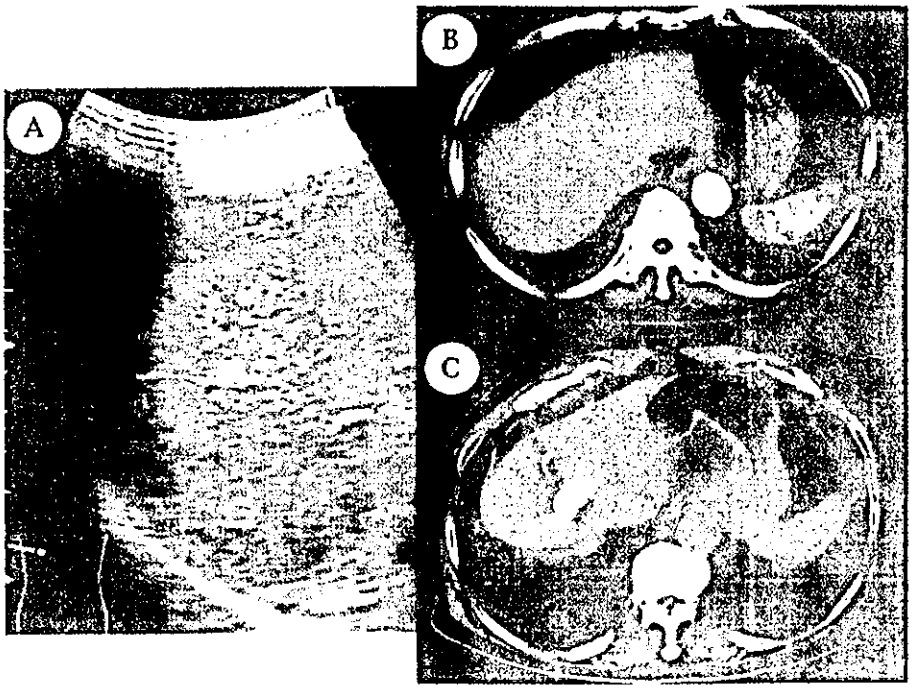

Figure 3. US and CT images of HCC (2.5 cm) located in the S8 region of the liver. Although the HCC was not detected by US before PELIT (A), it was clearly demonstrated by dynamic CT (B). PELIT was performed under the US guidance based on the judgment of the CT findings. Accumulation of lipiodol in the whole tumor was observed by plain CT (C).

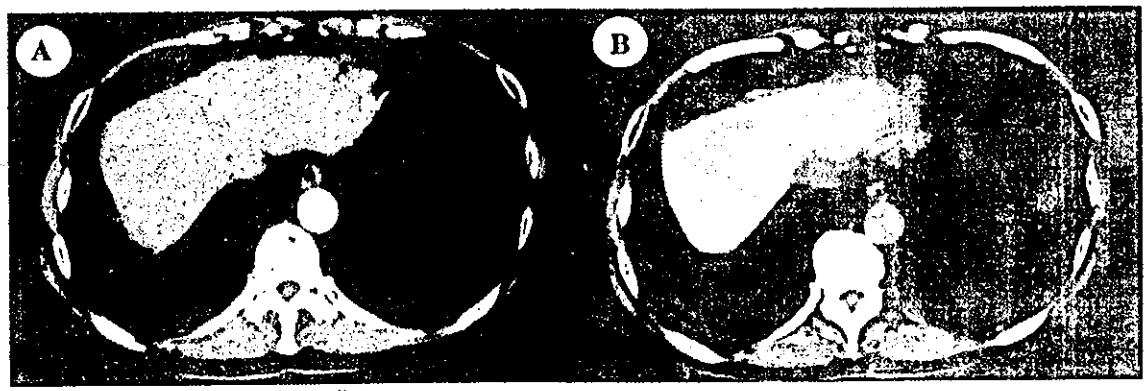

Figure 4. Contrast-enhanced dynamic CT before (A) and plain CT immediately after (B) PELIT for HCC (2 cm) located in the S4 region immediately under the diaphragm. In this case, the tumor was not visible by US. After PELIT, the area of lipiodol-deposit covered the entire tumor and reached beyond the tumor margin.

with the platelet count of 40,000/mm^3 and hepaplastin test of <50%. Because these conditions were considered not to be adaptable to RFA therapy, PELIT was performed in the tumor. This HCC showed no early enhancement (Fig. 5A), but was visible as a defect in the late phase of the dynamic CT (Fig. 5B), indicating that this tumor was hypovascular. In contrast, this tumor was sufficiently visible by US. After the initial treatment of PELIT, the mixture of lipiodol-ethanol was clearly accumulated in the entire tumor lesion (Fig. 5C). Seven months after the first PELIT, another HCC (2.5 cm in diameter) emerged in the S1 lesion of the liver. This tumor showed the enhancement in the early phase (Fig. 5D) and the defect in the late phase (Fig. 5E) of dynamic CT. Although the first tumor was hypovascular, the second one was shown to be hypervascular. Therefore, in this patient, 2 types of HCC with different vascularity emerged in different locations of the liver. The good accumulation of lipiodol was observed in the S7 region, even 7 months after PELIT, indicating that the deposit of lipiodol was kept stable in HCC for many months. The newly developed tumor in the S1 lesion was located close to the inferior vena cava and the portal tract, which prevented the insertion of a 17-gauge RFA electrode. Therefore, PELIT using a 21-gauge PEI needle was performed and 29 ml of the mixture of ethanol-lipiodol was injected into the tumor in 3 sessions of treatment. The deposit of ethanol-lipiodol covered the entire tumor (Fig. 5F). With PELIT for both tumors, no severe liver dysfunction was observed.

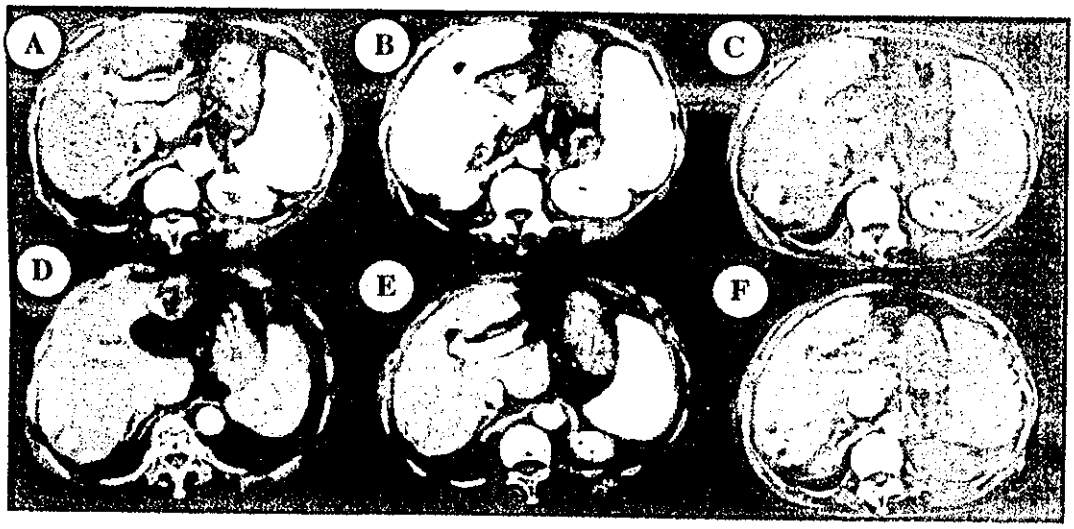

Figure 5. CT images of HCCs with hypo- and hyper-vascularity developed at different times in the same patient. The first HCC, 2.5 cm in diameter, was developed in the S7 region of the liver. The lesion did not show the early enhancement (A) but showed the defect (B) in the late phase of CT, indicating the hypovascularity of this tumor. After PELIT, plain CT revealed that the entire lesion was covered with lipiodol (C). Seven months after PELIT, the new lesion, 3 cm in diameter, was detected in the S1 region. The lesion showed early enhancement (D) and relatively low density (E) in the late phase of dynamic CT. After PELIT, plain CT showed that the entire tumor in the S1 region was covered with lipiodol along with the lipiodol-deposit in the S7 region (F).

Discussion

The strategy for the treatment of HCC has rapidly been shifting from surgical to non-surgical modalities by the introduction of RFA therapy in clinical settings. One reason for this shift is that RFA is able to achieve certain therapeutic effects on HCC in a few sessions of treatment without serious side effects. Although PEI therapy has been shown to be useful for the treatment of HCC, its efficacy is limited to relatively small-sized encapsulated lesions. In contrast, RFA therapy is applicable to patients with relatively large-sized HCCs, because RFA therapy is able to obtain an adequate safety margin around the tumor (27). We have recently reported the usefulness of the combination therapy of PEI and RFA (PEI-RFA). This strategy can enhance the effectiveness of the treatment for HCCs, especially for large-sized HCCs and those located in the regions that are difficult to treat with RFA (23-25). However, we have to face also cases that are difficult to treat with PEI-RFA or RFA alone for several reasons. For instance, if HCCs are located near the inferior vena cava, the portal tract, the gallbladder or the bile tract, these structures may prevent the insertion of a relatively thick RFA electrode. If HCCs develop in patients with severely impaired hepatic reserve, RFA therapy may cause unacceptable hepatic damage, such as hepatic failure. Furthermore, it s difficult to treat with RFA such HCCs that are not clearly visible by US or CT. In the present study, we have shown the effectiveness of PELIT, a combination therapy of ethanol injection and lipiodol injection, on such HCCs. We have also shown representative cases that were difficult to treat with RFA and successfully treat with PELIT. For the treatment of HCCs, several options of combination therapies have been reported such as transcatheter arterial embolization plus RFA and saline injection plus RFA (28-35). To our knowledge, this is the first report describing the effectiveness of the combination therapy of ethanol and lipiodol injection (PELIT) for the treatment of HCC, although a few reports suggested the usefulness of lipiodol-ethanol injection therapy (36).

In all cases examined in the present study, the injected ethanol-lipiodol was homogeneously accumulated in the tumor. It was shown that PELIT alone could successfully treat HCCs, because the foci with the early enhancement indicated by CT before the treatment completely disappeared. No side effects other than mild reversible liver dysfunction were observed. Importantly, local recurrence rates after PELIT were shown to be quite low in a short-term follow-up ranging from 4 to 15 months, indicating that the viable cells in the tumor were completely destroyed by the injection of ethanol-lipiodol. Because lipiodol was mixed with ethanol at a ratio of 1:10, it should be confirmed whether the cells in the region corresponding to the lipiodol deposit were completely destroyed by the PELIT. Thus, a liver biopsy was performed from the lipiodol-deposit region and whole HCC cells were confirmed to be necrotic by PELIT. Taken collectively, these results suggest that PELIT is effective for destroying the entire tumorous legion corresponding to the lipiodol deposit without major complications.

As shown in the present study, PELIT is likely to be especially useful for the treatment of tumors that are not clearly visible by US or CT, because the treated region with accumulated lipiodol can thereafter be easily confirmed not by contrast-enhanced CT but by plain CT. As shown in Figs. 4 and 5, the deposit of injected lipiodol was observed in hypovascular tumors as well as hypervascular ones. So far, lipiodol has been used with an anti-cancer drug in transcatheter arterial chemolipiolization. In this kind of use, the mixture of anti-cancer drug and lipiodol is not deposited in hypovascular tumors, implying that lipiodol does not work effectively on hypovascular tumors in the transcatheter arterial approach. In this regard, PELIT, a percutaneous administration of lipiodol, is thought to be useful for the treatment of tumors irrespective of the vascularity.

In the present study, we could confirm that lipiodol percutaneously injected into the HCCs had strong affinity with viable cells. Therefore, PELIT may be useful for the detection and treatment of the residual foci after RFA therapy. In fact, 2 cases (patients no. 4 and 7) of local recurrence after RFA therapy were successfully treated with PELIT and the effects have been sustained for over a year. The tight affinity of lipiodol with cancer cells may be helpful for other metastatic liver cancers as well.

RFA therapy is a very attractive and effective therapy for large-sized HCCs. In a sense, RFA therapy appears to be a radical treatment able to destroy the large area of the tumor in the liver. In contrast, PELIT appears to be a much milder therapy compared with RFA. Thus, the effects induced by PELIT are less invasive to the non-tumorous region in the liver, implying that this therapy is safer and milder than RFA therapy. The question may be raised why the usefulness of PELIT should be noted, when we have obtained the RFA technology. However, we believe that PELIT can play a certain role in the treatment of HCC because of its lesser invasiveness, and its convenience and dexterity. Therefore, the combined use of RFA therapy and PELIT according to the clinical status of patients or tumors may be useful for the treatment of HCCs, and this combination therapy may be able to diminish the difficulties and open up a new avenue in the treatment of HCCs.

Acknowledgments

The authors would like to dedicate this paper particularly to the memory of Ms. Natsuko Shimada, who was one of the patients with HCC and died of hepatic failure as a result of liver cirrhosis at our hospital on April 14, 2003. She was one of the patients who highly wished the development of our technologies for the treatment of HCC. This work was supported in part by Grant-in-Aid for Scientific Research (B-14370185 and C-14570473) from the Japanese Ministry of Education, Culture, Sports, Science and Technology.

References

1. Kuriyama S, Yamazaki M, Mitoro A, Tsujimoto T, Kikukawa M, Okuda H, Tsujinoue, H, Nakatani T, Yoshiji H, Toyokawa Y, Nagao S and Fukui H: Analysis of intrahepatic invasion of hepatocellular carcinoma using fluorescent dye-labeled cells in mice. Anticancer Res 18: 4181-4188, 1998.
2. Kuriyama S, Yamazaki M, Mitoro A, Tsujimoto T, Kikukawa M, Tsujinoue H, Nakatani T, Toyokawa Y, Yoshiji H and Fukui H: Hepatocellular carcinoma in an orthotopic mouse model metastasizes intrahepatically in cirrhotic but not in normal liver. Int J Cancer 80: 471-476, 1999.
3. Tsujimoto T, Kuriyama S, Yamazaki M, Nakatani Y, Okuda H, Yoshiji H and Fukui H: Augmented hepatocellular carcinoma progression and depressed Kupffer cell activity in rat cirrhotic livers. Int J Oncol 18: 41-47, 2001.
4. Venook AP: Treatment of hepatocellular carcinoma: too many options? J Clin Oncol 12: 1323-1334, 1994.
5. Colleoni M, Gaion F, Liessi G, Mastropasqua G, Nelli P and Manente P: Medical treatment of hepatocellular carcinoma: any progress? Tumori 80: 315-326, 1994.
6. Kuriyama S, Yoshikawa M, Ishizaka S, Tsujii T, Ikenaka K, Kagawa T, Morita N and Mikoshiba K: A potential approach for gene therapy targeting hepatoma using a liver-specific promoter on a retroviral vector. Cell Struct Funct 16: 503-510, 1991.
7. Kuriyama S, Nakatani T, Masui K, Sakamoto T, Tominaga K, Yoshikawa M, Fukui H, Ikenaka K and Tsujii T: Bystander effect caused by suicide gene expression indicates the feasibility of gene therapy for hepatocellular carcinoma. Hepatology 22: 1838-1846, 1995.
8. Cao G, Kuriyama S, Du P, Sakamoto T, Kong X, Masui K and Qi Z: Complete regression of established murine hepatocellular carcinoma by *in vivo* tumor necrosis factor a gene transfer. Gastroenterology 112: 501-510, 1997.
9. Kuriyama S, Sakamoto T, Masui K, Nakatani T, Tominaga K, Kikukawa M, Yoshikawa M, Ikenaka K, Fukui H and Tsujii T: Tissue-specific expression of HSV-tk gene can induce efficient antitumor effect and protective immunity to wild-type hepatocellular carcinoma Int J Cancer 71: 470-475, 1997.
10. Kuriyama S, Kikukawa M, Masui K, Okuda H, Nakatani T, Sakamoto T, Yoshiji H, Fukui H, Ikenaka K, Mullen CA and Tsujii T: Cytosine deaminase/5-fluorocytosine gene therapy can induce efficient anti-tumor effects and protective immunity in immunocompetent mice but not in athmic nude mice. Int J Cancer 81: 592-597, 1999.
11. Kuriyama S, Kikukawa M, Masui K, Okuda H, Nakatani T, Akahane T, Mitoro A, Tominaga K, Tsujinoue H, Yoshiji H, Okamoto S, Fukui H and Ikenaka K: Cancer gene therapy with HSV-tk/GCV system depends on T-cell-mediated immune responses and causes apoptotic death of tumor cells. Int J Cancer 83: 374-380, 1999.
12. Kuriyama S, Masui K, Kikukawa M, Sakamoto T, Nakatani T, Nagao S, Yamazaki M, Yoshiji H, Tsujinoue H, Fukui H, Yoshimatsu T and Ikenaka K: Complete cure of established murine hepatocellular carcinoma is achievable by repeated injections of retroviruses carrying the herpes simplex virus thymidine kinase gene. Gene Ther 6: 525-533, 1999.
13. Nakatani T, Kuriyama S, Tominaga K, Tsujimoto T, Mitoro A, Yamazaki M, Tsujinoue H, Yoshiji H, Nagao S and Fukui H: Assessment of efficiency and safety of adenovirus mediated gene transfer into normal and damaged murine livers. Gut 47: 563-570, 2000.
14. Nagao S, Kuriyama S, Okuda H, Tominaga K, Nakatani T, Tsujinoue H, Yoshiji H and Fukui H: Adenovirus-mediated gene transfer into tumors: evaluation of direct readministration of an adenoviral vector into subcutaneous tumors of immuno-competent mice. Int J Oncol 18: 57-65, 2001.
15. Tsujinoue H, Kuriyama S, Nakatani T, Yoshiji H, Akahane T, Toyokawa Y, Fukui H, Yoshimatsu T and Ikenaka K: Amelioration of retrovirus-mediated gene transfer into hepatocellular carcinoma cells. Int J Oncol 18: 801-807, 2001.
16. Kuriyama S, Mitoro A, Tsujinoue H, Nakatani T, Yoshiji H, Tsujimoto T, Yamazaki M and Fukui H: Particle-mediated gene transfer into murine livers using a newly developed gene gun, Gene Ther 7: 1132-1136, 2000.
17. Nagata Y, Hiraoka M, Akuta K, Abe M, Takahashi M, Jo S, Nishimura Y, Masunaga S, Fukuda M and Imura H: Radio-frequency thermotherapy for malignant liver tumors. Cancer 65: 1730-1736, 1990.
18. Allgaier HP, Deibert P, Zuber I, Olschewski M and Blum HE: Percutaneous radiofrequency interstitial thermal ablation of small hepatocellular carcinoma. Lancet 353: 1999.
19. Goldberg SN, Gazelle GS, Solbiati L, Livraghi T, Tanabe KK, Hahn PF and Mueller PR: Ablation of liver tumors using percutaneous RF therapy. Am J Roentgenol 170: 1023-1028, 1998.
20. Curley SA, Izzo F, Ellis LM and Vauthey NJ: Radio-frequency ablation of hepatocellular cancer in 110 patients with cirrhosis. Ann Surg 232: 381-391, 2000.
21. Solbiati L, Goldberg SN, Ierace T, Livraghi T, Meloni F, Dellanoce M, Sironi S and Gazelle GS: Hepatic metastases: percutaneous radio-frequency ablation with cooled-tip electrodes. Radiology 205: 367-372, 1997.
22. Solbiati L, Lerace T, Goldberg SN, Sironi S, Livraghi T, Fiocca R, Servadio G, Rizzatto G, Mueller PR, Del Maschio A and Gazelle GS: Percutaneous US-guided radio-frequency tissue ablation of liver metastases: treatment and follow-up in 16 patients. Radiology 202: 195-203, 1997.
23. Kurokohchi K, Watanabe S, Masaki T, Hosomi N, Funaki T, Arima K, Yoshida S, Miyauchi Y and Kuriyama S: Combined use of percutaneous ethanol injection and radiofrequency ablation for the effective treatment of hepatocellular carcinoma, Int J Oncol 21: 841-846, 2002.

24. Watanabe S, Kurokohchi K, Masaki T, Miyauchi Y, Funaki T, Inoue H, Himoto T, Kita Y, Uchida N, Touge T, Tatsukawa T and Kuriyama S: Enlargement of thermal ablation zone by the combination of ethanol injection and radiofrequency ablation in excised bovine liver. Int J Oncol 24: 279-284, 2004.
25. Kurokohchi K, Watanabe S, Masaki T, Hosomi N, Funaki T, Arima K, Yoshida S, Nakai S, Murota M, Miyauchi Y and Kuriyama S: Combination therapy of percutaneous ethanol injection and radiofrequency ablation against hepatocellular carcinomas difficult to treat. Int J Oncol 21: 611-615, 2002.
26. Kosari K, Gomes M, Hunter D, Hess DJ, Greeno E and Sielaff TD: Local, intrahepatic, and systemic recurrence patterns after radiofrequency ablation of hepatic malignancies. J Gastrointest Surg 6: 255-263, 2002.
27. Livraghi T, Goldberg SN, Lazzaroni S, Meloni F, Ierace T, Solbiati L and Gazelle GS: Hepatocellular carcinome: radiofrequency ablation of medium and large lesions. Radiology 214: 761-768, 2000.
28. Rossi S, Garbagnati F, Lencioni R, Allgaier H-P, Marchiano A, Fornari F, Quaretti P, Di Tolla G, Ambrosi C, Mazzaferro V, Blum HE and Bartolozzi C: Percutaneous radio-frequency thermal ablation of nonresectable hepatocellular carcinoma after occlusion of tumor blood supply. Radiology 217: 119-126, 2000.
29. Buscarini L, Buscarini E, Di Stasi M, Quaretti P and Zangrandl A: Percutaneous radiofrequency thermal ablation combined with transcatherter arterial embolization in the treatment of large hepatocellular carcinoma. Ultraschall Med 20: 47-53, 1999.
30. Okano H, Shiraki K, Inoue H, Ito T, Yamanaka T, Deguchi M, Sugimoto K, Sakai T, Ohmori S, Murata K, Takase K and Nakano T: Combining trascatheter arterial chemoembolization with percutaneous ethanol injection therapy for small size hepatocellular carcinoma. Int J Oncol 19: 909-912, 2001.
31. Yasuda S, Ito H, Yoshikawa M, Shinozaki M, Goto N, Fujimoto H, Nasu K, Uno T, Itami J, Isobe K, Shigematsu N, Ebara M and Saisho H: Radiotherapy for large hepatocellular carcinoma combined with transcatheter arterial embolization and percutaneous ethanol injection therapy. Int J Oncol 15: 467-473, 1999.
32. Yamasaki T, Kurokawa F, Shirahashi H, Kusano N, Hironaka K and Okita K: Percutaneous radiofrequency ablation therapy with combined angiography and computed tomography assistance for patients with hepatocellular carcinoma. Cancer 91: 1342-1348, 2001.
33. Kohda H, Sekiya C, Kanai M, Yoshida Y, Uede T, Kikuchi K, and Namiki M: Flow cytometric and functional analysis of mononuclear cells infiltrating the liver in experimental autoimmune hepatitis. Clin Exp Imunol 82: 473-478, 1990.
34. Livraghi T, Goldberg SN, Monti F, Bizzini A, Lazzaroni S, Meloni F, Pellicano S, Solbiati L and Gazelle GS: Saline-enhanced radio-frequency tissue ablation in the treatment of liver metastases. Radiology 202: 205-210, 1997.
35. Honda N, Guo Q, Uchida H, Ohishi H and Hiasa Y: Percutaneous hot saline injection therapy for hepatic tumors: an alternative to percutaneous ethanol injection therapy. Radiology 190: 53-57, 1994.
36. Tateishi H, Oi H, Masuda N, Yano H, Matsui S, Kinuta M, Maruyama H, Yayoi E and Okamura J: Appraisal of combination treatment for hepatocellular carcinoma: long-term follow-up and lipiodol percutaneous ethanol injection therapy. Semin Oncol 24 (Suppl. 6): 81-90, 1997.

Expression of G1 phase-related cell cycle molecules in naturally developing hepatocellular carcinoma of Long-Evans Cinnamon rats

YUKO KITA[1], TSUTOMU MASAKI[1], FUMI FUNAKOSHI[1], SHUHEI YOSHIDA[1], MISUZU TANAKA[1], KAZUTAKA KUROKOHCHI[1], NAOHITO UCHIDA[1], SEISHIRO WATANABE[1], KOZO MATSUMOTO[2] and SHIGEKI KURIYAMA[1]

[1]Third Department of Internal Medicine, Kagawa University School of Medicine, 1750-1 Ikenobe, Miki-cho, Kita-gun, Kagawa 761-0793; [2]Institute for Experimental Animal, University of Tokushima School of Medicine, 3-18-15 Kuramoto-cho, Tokushima, Tokushima 770-8503, Japan

Received December 12, 2003; Accepted February 10, 2004

Abstract. It has been shown that a variety of cell cycle-related proteins play important roles in the process of carcinogenesis including hepatocarcinogenesis. In the present study, we evaluated mRNA and protein expression of G1 phase-related cell cycle molecules in the process of hepatocarcinogenesis, using Long-Evans Cinnamon (LEC) rats, an animal model of hepatocellular carcinoma (HCC). The expression of cyclin D1, cyclin-dependent kinase 4 (Cdk4) and Cdk6 was measured quantitatively by real-time polymerase chain reaction. Cyclin D1 mRNA expression was increased significantly in chronic hepatitis liver compared with normal liver, and then decreased in HCC and the surrounding precancerous liver of LEC rats. Levels of Cdk4 mRNA were increased significantly in HCC compared to precancerous and chronic hepatitis livers. In contrast, mRNA levels of Cdk6 did not change significantly during hepatocarcinogenesis. We also evaluated the protein levels of these G1 phase-related cell cycle molecules by Western blot analyses and confirmed similar results. Total amounts of retinoblastoma protein (pRb) in the liver did not change significantly in the process of hepatocarcinogenesis in LEC rats. However, levels of phosphorylated pRb were increased markedly in the process of hepatocarcinogenesis, and the highest in HCC compared to precancerous, chronic hepatitis and normal livers. These results indicate that cyclin D1 may be involved in the regeneration of hepatocytes rather than hepatocarcinogenesis, while Cdk4 but not Cdk6 may play an important role in the development of HCC.

Correspondence to: Dr Shigeki Kuriyama, Third Department of Internal Medicine, Kagawa University School of Medicine, 1750-1 Ikenobe, Miki-cho, Kita-gun, Kagawa 761-0793, Japan
E-mail: skuriyam@kms.ac.jp

Key words: cell cycle, hepatocarcinogenesis, hepatocellular carcinoma, G1 phase, cyclin D1, cyclin-dependent kinase, retinoblastoma

Introduction

The inbred strain of Long-Evans Cinnamon (LEC) rats was established as a mutant strain that spontaneously suffers from chronic liver injury and subsequently develops hepatocellular carcinoma (HCC) (1,2). Severe acute hepatitis with jaundice spontaneously develops in LEC rats 4-5 months after birth. Approximately 30-40% of LEC rats die of fulminant hepatitis, and the remaining ones suffer from chronic hepatitis for life. Almost all LEC rats develop HCC when they are 18-months-old (3,4). It has been confirmed that abnormal copper accumulation occurs in the liver of LEC rats and that the occurrence of liver injury is linked genetically (5,6). Because the natural history of liver disease in LEC rats closely resembles that of human hepatic diseases in which HCC follows persistent hepatitis, LEC rats are regarded as a useful animal model for the research of the mechanisms of human hepatocarcinogenesis.

Cyclins and their catalytic subunits, cyclin-dependent kinases (Cdks), play pivotal roles in the regulation of cell cycle events (7). Cdks control the passage through the restriction point and entry into S phase. Cdks are sequentially regulated by cyclins A, D and E. Among the cyclins, D-type cyclin is the primary regulator and is absolutely required for cellular progression through G1 phase of the cell cycle (8-10). Specific cyclin/Cdk complexes are activated at different intervals during the cell cycle. Cyclin D1/Cdk4 and cyclin D1/Cdk6 are activated in mid-G1 phase. The activation of cyclin D1/Cdk4 and cyclin D1/Cdk6 complexes is responsible for the phosphorylation of retinoblastoma protein (pRb), the ultimate substrate in the pathway leading to transition from G1 to S phase. Thus, G1 phase-related cell cycle molecules play essential roles in the entry into the cell cycle.

In the present study, to examine the involvement of G1 phase-related cell cycle molecules in hepatocarcinogenesis, we assessed mRNA expression of cyclin D1, Cdk4 and Cdk6